Order Number 1350390

Comparison of interface trap measurements in high field stressed MOS transistors

Todsen, James Lee, M.S.

The University of Arizona, 1992

U·M·I
300 N. Zeeb Rd.
Ann Arbor, MI 48106

COMPARISON OF INTERFACE TRAP MEASUREMENTS IN HIGH FIELD STRESSED MOS TRANSISTORS

by
James Lee Todsen

A Thesis Submitted to the Faculty of the

DEPARTMENT OF ELECTRICAL AND COMPUTER ENGINEERING

In Partial Fulfillment of the Requirements
For the Degree of

MASTER OF SCIENCE
WITH A MAJOR IN ELECTRICAL ENGINEERING

In the Graduate College

THE UNIVERSITY OF ARIZONA

1992

STATEMENT BY AUTHOR

This thesis has been submitted in partial fulfillment of requirements for an advanced degree at The University of Arizona and is deposited in the University Library to be made available to borrowers under rules of the Library.

Brief quotations from this thesis are allowable without special permission, provided that accurate acknowledgement of source is made. Requests for permission for extended quotation from or reproduction of this manuscript in whole or in part may be granted by the copyright holder.

SIGNED: James Lee Tobler

APPROVAL BY THESIS DIRECTOR

This thesis has been approved on the date shown below:

R. D. Schrimpf — 8/7/92

Ronald D. Schrimpf
Associate Professor of
Electrical and Computer Engineering

Date

ACKNOWLEDGEMENTS

I would like to thank my wife Ae for her love, patience and support as I worked on this thesis. Also, I would like to thank my family for their continued support and encouragement.

I am indebted to Dr. Ron Schrimpf and Dr. Ken Galloway for the expertise and guidance they provided throughout my work. A special thanks is extended to Bob Craigin from the University of Arizona and Dave Wayne, Gerry Harder and Paul Gerrish from Micro-Rel in Tempe, AZ, for their generous assistance in packaging the experimental devices. I would like to thank Pascal Augier for his work in designing and building the $1/f$ noise measurement system. He and the rest of the Radiation Effects Group were always a great resource for me.

Finally, I would like to acknowledge the Defense Nuclear Agency for their generous support that made possible this project.

TABLE OF CONTENTS

LIST OF FIGURES

LIST OF FIGURES CONTINUED

ABSTRACT

The effects of high field stress on interface trap densities (D_{it}) in MOS transistors are compared using three methods: charge-pumping, subthreshold swing and $1/f$ noise. The experimental MOS devices subjected to high field stress originated from two wafer lots processed with different concentrations of copper in the buffered oxide etchant. For the charge-pumping and subthreshold methods, no dependency is found on stress current polarity, wafer lot or transistor type (n- or p-channel). These two methods yield similar D_{it} values. For the $1/f$ noise method, no dependency is found on current polarity or wafer lot. However, the noise in the n-channel devices increases by several orders of magnitude as compared to the p-channel devices. A large discrepancy is found between D_{it} calculated from $1/f$ noise when compared to charge-pumping/subthreshold swing results for n-channel transistors For p-channel transistors, the $1/f$ D_{it} results are in much better agreement with the results of the other two methods.

CHAPTER 1

INTRODUCTION

The Si-SiO_2 interface in a MOS device interrupts the periodic nature of the silicon lattice. As a result of this interface, broken or "dangling" bonds form. Figure 1.1 shows a simplistic representation of the interface bonding structure. These "dangling" bonds are believed to create the electronic traps known to exist at the interface. These traps, often referred to as interface traps, interface states or surface states, introduce energy levels within the silicon bandgap. Carriers in the semiconductor are then free to interact with these levels.

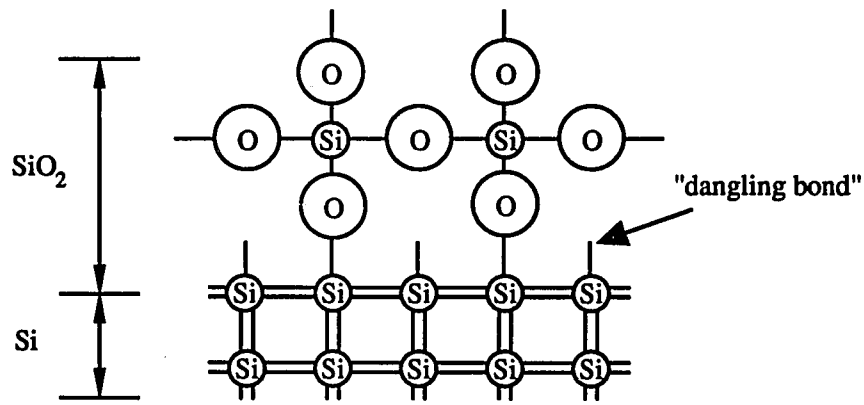

Figure 1.1 Simplified view of interface traps as "dangling bonds" due to mismatch between Si and SiO_2 lattices (after Deal [1]).

The control of the interface trap density D_{it} was a very significant problem during the development of the MOS transistor. High levels of interface states present in the first experimental devices drastically affected their performance [2]. As research continued, improvements in processing allowed a SiO_2 layer to be grown on the silicon substrate with few traps at the interface. This ability to control D_{it} in the Si-SiO_2 interface was in fact one of the key factors in helping this particular technology to become so dominant [3].

Today, the annealing process steps incorporated in the fabrication flow of MOS devices greatly reduce D_{it}. However, under certain conditions such as high field stress, hot carrier injection and exposure to ionizing radiation, the level of interface traps significantly increases. Device degradation resulting in lower transconductances and mobilities, threshold voltage shifts and increased device capacitance also occurs under the previously mentioned conditions. Correlating the observed degradation to D_{it} under these conditions requires an accurate means of measuring the interface trap density.

A variety of methods have been presented in the literature to measure D_{it}. Most of these methods directly measure device capacitance and are principally used with MOS capacitors. The capacitance, which is proportional to area, of MOS transistors is usually too small to be accurately measured. Methods more suitable for use with the smaller transistor structures have been developed using different techniques. The purpose of this thesis is to examine interface trap creation due to high field stress using three of these methods:

Charge-Pumping

Subthreshold-Swing

1/*f* Noise.

The three methods compared in this thesis use different characteristics of the interface traps in determining D_{it}. The charge-pumping method forces carriers into and out of the channel under the presence of an oscillating gate voltage. Carriers are trapped in the interface states during the first phase of the gate oscillation, then recombine in the second phase, generating a net substrate current which is proportional to D_{it}. The subthreshold swing method measures the additional capacitance in the subthreshold regime added by the interface traps. The additional capacitance is detected via changes in the gate-voltage swing. The third method, $1/f$ noise, is somewhat controversial due to disagreements over the origin of the noise. This thesis assumes the noise is due to fluctuations in the number of carriers in the channel resulting from the carriers quantum mechanical tunneling to traps at or near the interface.

In order to evaluate the three methods for measuring D_{it} listed above, n- and p-channel MOS transistors were subjected to high field stress by forcing a constant current into the transistor's gate. During the experiments, the stressing was periodically interrupted and all three measurements performed. Currents of both positive and negative polarities were used on devices from two different wafer lots. The wafer lots were processed in conjunction with the University of Arizona SEMATECH Center of Excellence for Contamination/Defect Assessment and Control.

Chapter 2 provides an overview of the theory behind the three methods for measuring D_{it} as well as a brief discussion of high field stressing. The experimental details are given in Chapter 3. Chapter 4 presents the experimental results with discussion. Finally, in Chapter 5, the thesis is summarized and concluding remarks are given. Appendices A and B provide a detailed description of the test setups used in this thesis for the $1/f$ noise and charge-pumping measurements.

CHAPTER 2

THEORETICAL OVERVIEW

This chapter presents a brief overview of the three methods used in this thesis for measuring D_{it} and a short discussion on high field stress. Only the key equations are given in describing the three methods since the complete explanations are quite lengthy. The reader is referred to the references given in each subsection for more detailed analyses.

2.1 Charge-Pumping

Charge-pumping was first introduced by Brugler and Jespers [4]. The basic setup for making the measurements appears in Figure 2.1. With the source and drain reverse biased with respect to the substrate, the gate of the transistor is swept between inversion and accumulation. During inversion, minority carriers supplied by the source and drain fill the channel of the transistor. Interface states trap some of these carriers. Driving the gate into accumulation forces the minority carriers to be swept out of the channel and into the reverse biased source and drain. Those carriers trapped in the interface states that are not swept out recombine during accumulation with the substrate's majority carriers, generating a net flow of charge into the substrate. This charge is commonly designated as the charge-pumping charge Q_{CP}. Repetitively sweeping the gate between inversion and

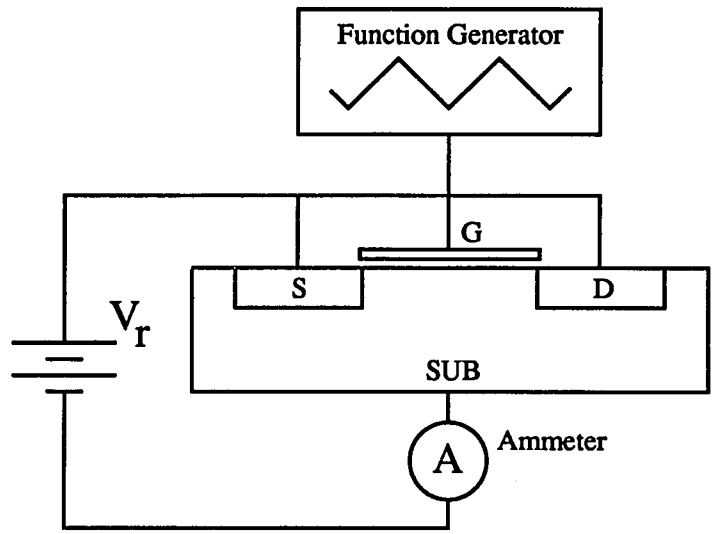

Figure 2.1 Simplified block diagram of charge-pumping setup. See Appendix B for a more complete description of the setup used in this thesis.

accumulation at a frequency f produces a charge-pumping current equal to

$$I_{CP} = fQ_{CP}. \tag{2.1}$$

Groeseneken et al. have carefully analyzed the nature of the currents flowing during a charge-pumping cycle and have derived an equation relating D_{it} to I_{CP} [5]. This equation provides the basis for a straightforward method of measuring D_{it} which has found wide-spread acceptance. Their approach is followed in this thesis and the principal equations are given below.

Four currents flow into and out of the interface traps during a charge-pumping cycle. Two of these currents result from minority carriers (I_1 and I_2 in Figure 2.2) while the other two are due to majority carriers (I_3 and I_4 in Figure 2.2). As the transistor enters

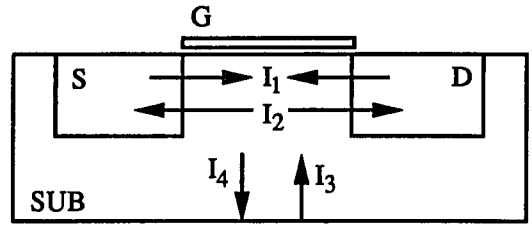

Figure 2.2 Diagram of the four currents flowing during one cycle of the gate triangle wave (after Groeseneken et al. [5]).

the inversion regime, minority carriers flow from the source and drain and fill the unoccupied traps: I_1. When the surface potential moves towards accumulation some of the trapped minority carriers are emitted back to the source and drain: I_2. The same type of process occurs for majority carriers during the accumulation period. The net flow of the majority carriers, $I_3 + I_4$, (or minority carriers $I_1 + I_2$) produces the charge-pumping current measured in the setup shown in Figure 2.1.

The above description of current flow during a charge-pumping cycle assumes that the free carriers in the channel have sufficient time to be removed during the transitions between inversion and accumulation. For very high gate signal frequencies or very low *W/L* (width/length) ratios, this assumption is not valid. An additional current, the so-called "geometric" component [5], flows due to the recombination of free carriers that do not have time to be swept from the channel. The current measured by the ammeter in Figure 2.1 is a summation of the ideal charge-pumping current and the geometric component. Therefore, in order to obtain accurate results from the charge-pumping method, there should be no geometric component present, or else it must be accounted for in the analysis.

By expanding the expression $I_3 + I_4$ with the appropriate terms, one can show that the charge-pumping current for a triangular gate wave with a 50% duty cycle and sufficient amplitude to drive the channel from accumulation to inversion is [5]

$$I_{CP} = f2qA_G D_{it} kT\left[\ln\left(\frac{v_{th} n_i}{2}\sqrt{\sigma_p \sigma_n}\frac{|V_{FB} - V_T|}{|V_{Gp-p}|}\right) - \ln(f)\right] \tag{2.2}$$

where

q is the electron charge (C)

A_G is the effective area of the channel under the gate (cm^2)

D_{it} is the average interface trap density in the bandgap ($cm^{-2}\,eV^{-1}$)

k is Boltzmann's constant (eV/K)

T is the absolute temperature (K)

f is the frequency (Hz)

v_{th} is the thermal velocity (cm/s)

n_i is the intrinsic carrier concentration (cm^{-3})

σ_p, σ_n are the hole and electron capture cross-sections (cm^2)

V_{FB} is the flatband voltage (V)

V_T is the threshold voltage (V)

$V_{Gp\text{-}p}$ is the peak-to-peak gate voltage (V).

Equation (2.2) assumes the transistor is n-channel. The charge-pumping charge can be obtained from I_{CP} using (2.1). Combining (2.1) and (2.2) we see that

$$Q_{CP} = 2qA_G kTD_{it}[\ln(C) - \ln(f)] \tag{2.3}$$

with C replacing the appropriate variables in (2.2).

The final step in the charge-pumping derivation is to take the derivative of Q_{CP} in (2.3) with respect to ln(f). Doing so yields

$$\frac{\partial Q_{CP}}{\partial \ln(f)} = -2qkTA_G D_{it}. \tag{2.4}$$

Taking the absolute value of (2.4) removes the negative sign from the right hand side of that equation so that

$$\left|\frac{\partial Q_{CP}}{\partial \ln(f)}\right| = 2qkTA_G D_{it}. \tag{2.5}$$

This last equation, (2.5), is easily rearranged so as to determine D_{it} from the slope of Q_{CP} versus ln(f). Note, the only device parameter needed to measure D_{it} with the charge-pumping method is the device area A_G. The interface trap density calculated using (2.5) is the average value of D_{it} over the bandgap. Figures 2.3 and 2.4 show typical n-channel device results for $|I_{CP}|$ versus f and $|Q_{CP}|$ versus ln(f), respectively.

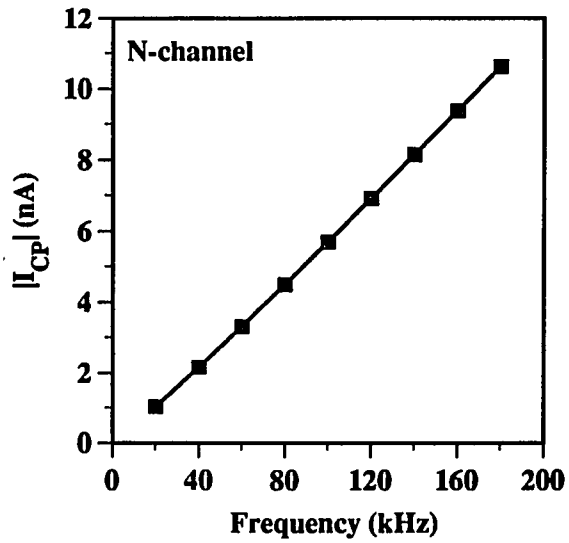

Figure 2.3 Frequency dependence of I_{CP}. The absolute value of I_{CP} is plotted since the measured values for a n-channel device are negative.

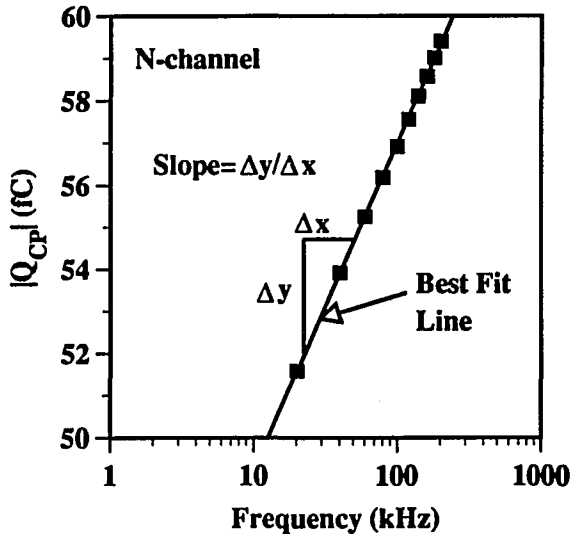

Figure 2.4 Log frequency dependence of Q_{CP}. The slope is used in (2.5) to determine D_{it}.

2.2 Subthreshold Swing

The subthreshold swing method, also known as the subthreshold slope method, extracts the interface trap density from the slope of the subthreshold log(I_D) versus V_{GS} characteristics. Interface traps create an additional capacitance C_{it} which distorts or "stretches" the subthreshold characteristics. Figure 2.5 illustrates the change in subthreshold characteristics due to additional interface traps. Knowing the depletion layer capacitance and the oxide capacitance allows C_{it} to be determined. This value is then used to calculate the interface trap density located in energy about the center of the subthreshold regime.

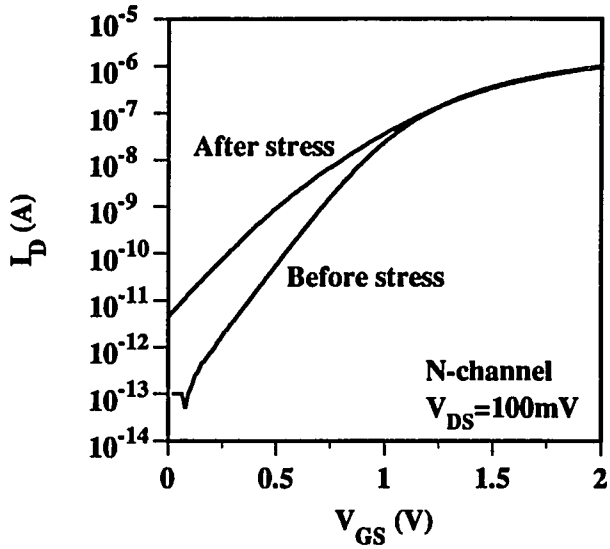

Figure 2.5 Subthreshold plots before and after constant current stressing. The increase in subthreshold swing, as defined by (2.8), after the stressing is due to the presence of additional interface states.

While in the subthreshold regime, a MOS transistor's drain current as a function of surface potential ψ_S (for a n-channel transistor) is given by [6]

$$I_D = \mu_n \left(\frac{W}{L}\right) \frac{aC_{ox}}{2\beta^2} \left(\frac{n_i}{N_A}\right)^2 \left(1 - e^{-\beta V_D}\right) e^{\beta \psi_S} (\beta \psi_S)^{-1/2} \tag{2.6}$$

where

μ_n is the effective mobility of electrons in the channel (cm^2/Vs)

W/L is the ratio of device width to length

a is a factor equal to $\sqrt{2}(\varepsilon_{Si} / L_D) / C_{ox}$

ε_{Si} is the permittivity of silicon (F/cm)

L_D is the Debye length (cm)

C_{ox} is the oxide capacitance (F/cm^2)

n_i is the intrinsic carrier concentration (cm^{-3})

N_A is the acceptor doping concentration (cm^{-3})

β is the inverse of the thermal voltage: $\frac{q}{kT}$ (V^{-1})

V_D is the drain voltage (V).

The surface potential expressed as a function of gate voltage is

$$\psi_S = (V_{GS} - V_{FB}) - \frac{a}{2\beta}\left\{\left[1 + \frac{4}{a^2}(\beta V_{GS} - \beta V_{FB} - 1)\right]^{1/2} - 1\right\} \tag{2.7}$$

where V_{FB} is the flatband voltage.

The subthreshold swing by definition is

$$S \equiv \frac{\partial V_{GS}}{\partial \log I_D}. \tag{2.8}$$

By combining (2.6) and (2.7) with (2.8), we can express the subthreshold swing as

$$S = (kT/q)\left[1 + C_D / C_{ox}\right]\left\{1 - \left(\frac{2}{a^2}\right)\left[C_D / C_{ox}\right]^2\right\}^{-1} \tag{2.9}$$

where C_D is the depletion layer capacitance (without interface traps) given by

$$C_D = \sqrt{\frac{q\varepsilon_{Si}N_A}{2\psi_S}}. \tag{2.10}$$

The capacitance associated with the interface traps C_{it} acts in parallel with the depletion layer capacitance. Assuming $a \gg (C_D / C_{ox})$ and substituting $(C_{it} + C_D)$ for C_D, (2.9) reduces to

$$S = (kT/q)\left[1 + (C_D + C_{it})/C_{ox}\right]. \tag{2.11}$$

This equation is easily solved for C_{it}. Dividing by q yields the following expression for D_{it} located in energy about the center of the subthreshold regime [7]

$$D_{it} = \frac{C_{it}}{q} = \frac{1}{q}\left[\left(S\frac{q}{kT} - 1\right)C_{ox} - C_D\right]. \tag{2.12}$$

Measuring the subthreshold swing is easy and takes little time. These desirable features are somewhat offset, however, by two limitations. First, in order to use (2.12), one must know the depletion and oxide capacitances. This in turn implies that the substrate doping level and the oxide thickness must be known. Unfortunately, (2.12) is sensitive to both of these parameters. Note, if all that is required is information on relative changes in D_{it}, then the subthreshold swing method can be used without knowing the substrate doping level as the depletion capacitance drops out of (2.12) when relative measurements are made. The second limitation arises from the assumptions used to derive the subthreshold swing equations. Long channel MOS transistor approximations were invoked. These equations are only accurate for long channel lengths ($\geq$ 20 μm [7]), therefore restricting this method to use on long channel devices.

2.3 1/*f* Noise

Since its discovery by Johnson in 1925 [8], 1/*f* noise has been intensely studied. The observance of 1/*f* type spectra in a large variety of systems, for example the period of the human heartbeat [9] and the height of the Nile River [10], has fueled considerable debate on the origins of the noise. For MOS devices, the presence of 1/*f* noise in MOS transistors, yet not in JFETs, strongly suggests that the noise is a surface effect. Of the many models presented to explain 1/*f* noise in MOS transistors, most fall into one of three categories:

Number Fluctuation models

Mobility Fluctuation models

Combinations of the first two models.

The number fluctuation model was originally proposed by McWhorter [11] and has since been refined [12]. The basic assumption of this model is that the carrier density in the channel fluctuates as the carriers tunnel into and out of traps at or near the Si-SiO_2 interface. Strong experimental support for this model has been presented [13-15]. The mobility fluctuation model based on Hooge's Law [16] attributes $1/f$ noise to fluctuations in mobility due to lattice and impurity scattering. This model does not consistently explain the results seen in MOS transistors and seems more applicable to homogeneous materials [17]. The intuitively appealing idea of combining the previous two theories has been presented by several authors. Some assume the number and mobility fluctuations are independent [18], while others have more recently considered a correlated model [19]. The disadvantage of this approach is that a closed-form solution is not available. For this thesis, the number fluctuation model was chosen based on its wide acceptance and its tractability.

As previously mentioned, the basic assumption of the number fluctuation model is that the carriers tunnel into and out of traps at or near the interface, resulting in a fluctuation in the number of carriers in the channel. The time constants for these traps obey an exponential dependence on distance into the oxide. A summation of all these traps, over volume and energy, leads to a $1/f$ spectrum. The derivation below for a n-channel transistor summarizes the work of Christensson et al. [12].

The power spectral density of the fluctuations in the number of trapped carriers in a volume/energy element $\Delta V \Delta E$ is given by

$$S_{N_T \Delta V \Delta E} = \frac{4\tau_T}{1+\omega^2\tau_T^2} N_t(x,E) f_T(1-f_T) \Delta V \Delta E \tag{2.13}$$

where

τ_T is the trap time constant (s)

N_t is the trap density ($cm^{-3}\ eV^{-1}$)

ω is the angular frequency (rad/s)

f_T is the Fermi function

$$f_T = \frac{1}{1+e^{\frac{E_T - E_{Fn}}{kT}}}. \tag{2.14}$$

E_T is the energy level of the traps

E_{Fn} is the electron quasi-Fermi energy level.

Figure 2.6 contains a definition of the coordinate system.

The time constant of a trap is determined by its distance from the interface. Assuming the oxide tunnel barrier seen by an inversion layer carrier is a rectangular barrier of height ϕ_B, the difference in conduction band heights between the oxide and the silicon, the time constants obey the exponential relationship

$$\tau_T = \tau_0 e^{\alpha x} \tag{2.15}$$

where τ_0 is the trap time constant for $x = 0$ and

$$\alpha = \frac{4\pi}{h}\sqrt{2m_e^* \phi_B}. \tag{2.16}$$

In (2.16), h is Planck's constant and m_e^* is the effective mass of an electron in the oxide. Assuming an electron barrier height of 3.2 eV and a hole barrier height of 4.7 eV, the values of α are $1.8 \times 10^8\ cm^{-1}$ for n-channel devices and $2.2 \times 10^8\ cm^{-1}$ for p-channel devices. Typically, it is assumed that $\tau_0 = 1 \times 10^{-10}$ s [19].

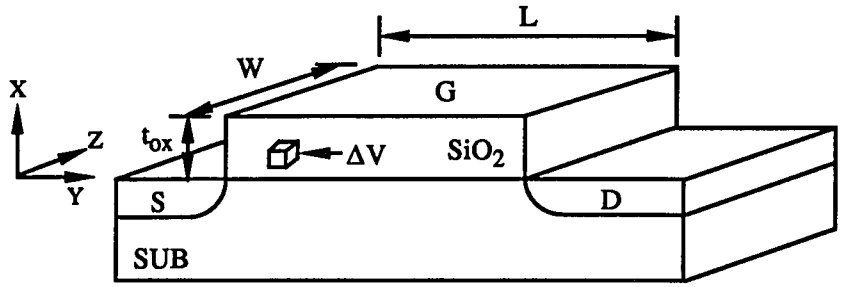

(a)

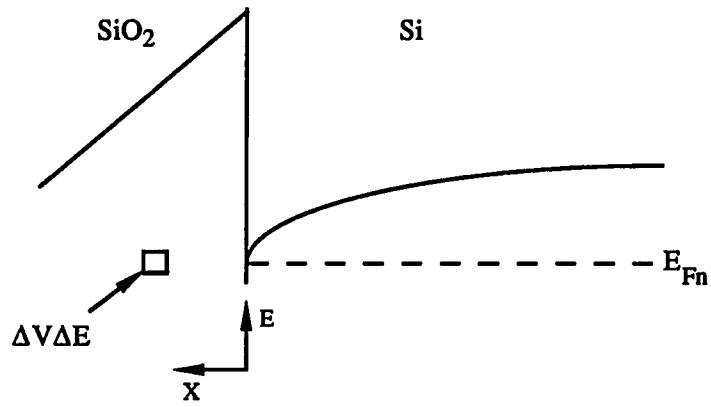

(b)

Figure 2.6 Definition of coordinate systems used in $1/f$ noise derivations in real (a) and energy (b) space. $\Delta V = \Delta x \Delta y \Delta z$ is a physical volume element and ΔE is an energy element. At the Si-SiO_2 interface $x = 0$ and at the source-channel interface $y = 0$. $E = 0$ at the bottom of the conduction band edge and increases with energy above E_c as measured under flatband conditions (after Jayarman and Sodini [19]).

Under the conditions of strong inversion, with $t_{ox} \gg d_t$ (d_t is the maximum tunneling distance into the oxide by the carriers in the channel), the power spectral density of the fluctuations in channel carriers is approximately equal to that of the carriers trapped so that

$$S_{Q_N \Delta V \Delta E} = q^2 S_{N_T \Delta V \Delta E}. \tag{2.17}$$

From basic MOS transistor theory, the drain current in the linear region (for a n-channel) device is

$$I_D = \mu_n \left(\frac{W}{L}\right) Q_N V_{DS} \tag{2.18}$$

with

$$Q_N = C_{ox}(V_{GS} - V_T). \tag{2.19}$$

The drain current fluctuation due to fluctuating channel carriers is then given by

$$\delta I_{D \Delta V \Delta E} = \mu_n \left(\frac{W}{L}\right) V_{DS} \frac{\delta Q_{N \Delta y \Delta z}}{WL}. \tag{2.20}$$

The factor $\frac{\delta Q_{N \Delta y \Delta z}}{WL}$ in (2.20) is the weighted value of the channel carrier fluctuations in an element $\Delta y \Delta z$.

The power spectral density of fluctuations in drain current is easily calculated from (2.20). Using the relationship shown in (2.17) gives the following expression

$$S_{I_D \Delta V \Delta E} = \frac{\mu_n^2 V_{DS}^2}{L^4} S_{Q_N \Delta V \Delta E} = \frac{\mu_n^2 V_{DS}^2}{L^4} q^2 S_{N_T \Delta V \Delta E}. \tag{2.21}$$

To find the drain noise spectrum, (2.21) is simply divided by the square of the channel conductance g_D so that

$$S_{V_D \Delta V \Delta E} = \frac{S_{I_D \Delta V \Delta E}}{g_D^2} = \frac{q^2 V_{DS}^2}{(WL)^2 C_{ox}^2 (V_{GS} - V_T)^2} S_{N_T \Delta V \Delta E}. \tag{2.22}$$

Note, (2.22) assumes that the channel resistance is much smaller than any external resistance connected to the drain in order to physically measure S_{V_D}. Substituting (2.13) and (2.19) into (2.22) we obtain

$$S_{V_D \Delta V \Delta E} = \frac{q^2 V_{DS}^2}{(WL)^2 C_{ox}^2 (V_{GS} - V_T)^2} \frac{4\tau_T}{1+\omega^2 \tau_T^2} N_t(x,E) f_T(1-f_T) \Delta V \Delta E. \tag{2.23}$$

All that remains is to integrate (2.23) with respect to ΔE and ΔV. The function $N_t f_T(1 - f_T)$ is strongly peaked about E_{Fn}, the quasi-Fermi level. The integral of this equation over the bandgap energy can be approximated by $4kTN_t(E_{Fn})$ where $N_t(E_{Fn})$ represents the trap density (cm^{-3} eV^{-1}) located in energy around the quasi-Fermi level [12]. Integration over y and z merely cancels a factor of WL in the denominator of (2.23). Performing these integrations on (2.23) we are left with

$$S_{V_D} = \frac{16kTq^2 V_{DS}^2}{(WL) C_{ox}^2 (V_{GS} - V_T)^2} N_t(E_{Fn}) \int_0^{d_t} \frac{\tau_T}{1+\omega^2 \tau_T^2} dx. \tag{2.24}$$

The variables x and τ_T are related as shown in (2.15). Changing the variable of integration in (2.24) from x to τ we see that

$$\int_0^{d_t} \frac{\tau_T(x)}{1+\omega^2 \tau_T^2(x)} dx = \int_{\tau_0}^{\tau(d_t)} \frac{\tau}{1+\omega^2 \tau^2} \frac{d\tau}{\alpha \tau}. \tag{2.25}$$

The integral on the right hand side of (2.25) is equal to

$$\frac{1}{\alpha\omega} \left(\tan^{-1} \omega\tau(d_t) - \tan^{-1} \omega\tau_0 \right). \tag{2.26}$$

Assuming $\omega\tau_0 \ll 1 \ll \omega\tau(d_t)$ - which is true for the frequency range used in this thesis, (2.26) reduces to $\frac{\pi}{2\alpha\omega} = \frac{1}{4\alpha f}$. Substituting this value for the integral over x in (2.24) leads to the final expression for S_{V_D}

$$S_{V_D} = \frac{4q^2 kTV_{DS}^2}{\alpha (WL) C_{ox}^2 (V_{GS} - V_T)^2} \frac{N_t(E_{Fn})}{f}. \tag{2.27}$$

Due to the influence of the peaked function $f_T(1 - f_T)$, only traps close ($\pm 2kT$) to the quasi-Fermi level contribute to the $1/f$ noise. Figure 2.7 shows this region or "window" in the oxide. By multiplying $N_t(E_{Fn})$ by the maximum tunneling distance d_t, the trap density in units of $cm^{-2}eV^{-1}$ about the quasi-Fermi level averaged over the tunneling distance into the oxide can be found. The maximum tunneling distance used to generate the data in Chapter 4 was assumed to be 10 Å which from (2.15) is seen to produce the needed time constant spread of the measured noise. Chapter 3 describes the noise measurement system.

Recasting (2.27) as

$$S_{V_D} = \frac{V_{DS}^2}{(V_{GS} - V_T)^2} \frac{K_{1/f}}{f} \tag{2.28}$$

with

$$K_{1/f} = \frac{4q^2 kTN_t(E_{Fn})}{\alpha(WL)C_{ox}^2} \tag{2.29}$$

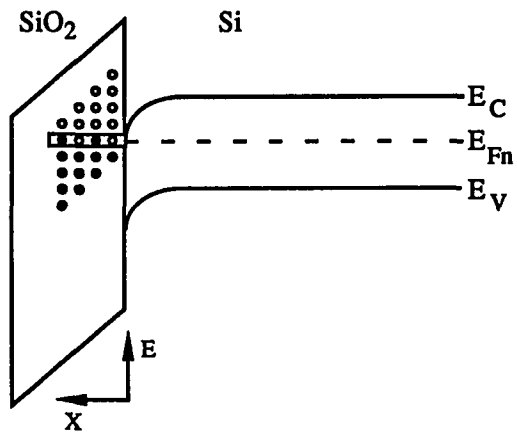

Figure 2.7 Diagram of "window" into oxide accessed in (x,E) space by $1/f$ noise measurements performed in the strong linear region.

provides an easy means of verifying the number fluctuation model. From (2.28) we see that the noise spectral density at a given frequency should be proportional to $(V_{GS} - V_T)^{-2}$ and to $(V_{DS})^2$. Figures 2.8 and 2.9 show S_{V_D} at f = 1 Hz versus $(V_{GS} - V_T)$ and V_{DS}. The measurements were made on a n-channel device with a $\left(\frac{W}{L}\right)$ ratio of $\left(\frac{5\ \mu m}{20\ \mu m}\right)$ using the setup described in Appendix A. The slopes of the curve fittings are shown in both figures. For Figure 2.8, theory predicts a slope of -2 and for Figure 2.9 theory predicts a slope of +2. As can be seen, reasonable agreement between the number fluctuation model predictions and experimental results is found.

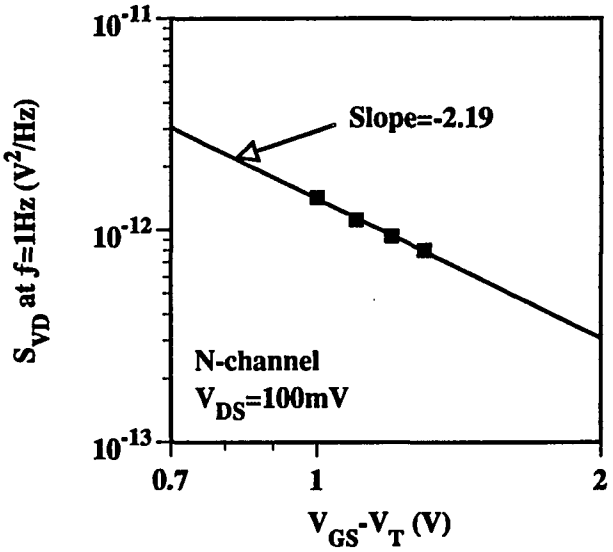

Figure 2.8 S_{V_D} at f = 1 Hz versus $(V_{GS} - V_T)$. Theory predicts a slope of -2.

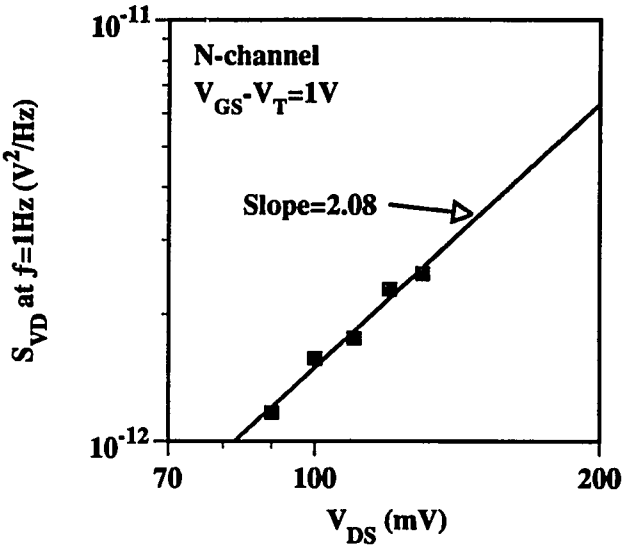

Figure 2.9 S_{V_D} at f = 1 Hz versus V_{DS}. Theory predicts a slope of +2.

2.4 High Field Stressing

High electric fields (E > 5 MV/cm) imposed across the oxide layer sharply bend the energy bands. This condition, commonly referred to as high field stressing, allows electrons to pass through the oxide via Fowler-Norheim (FN) tunneling [20]. Figure 2.10 shows the energy band diagram of a PMOS capacitor experiencing FN tunneling. It is assumed that holes do not participate in the tunneling process due to the larger barrier height they see.

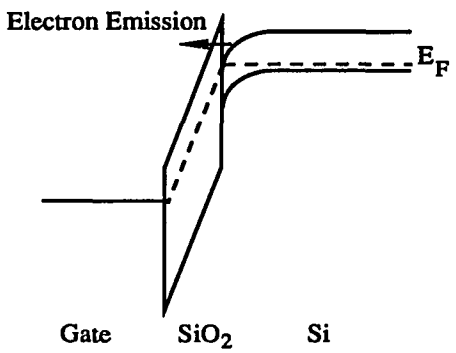

Figure 2.10 Energy band diagram of MOS capacitor during Fowler-Nordheim tunneling (after Lenzlinger and Snow [20]).

Electrically erasable programmable read-only memories (EEPROMs) use FN tunneling as a means of programming and erasing memory cells. In studying these devices, it has been observed that the FN tunneling in MOS devices creates additional interface traps as well as inducing trapped oxide charge [21]. For memory cells these phenomena are undesirable, however FN tunneling does provide an efficient means of increasing D_{it} in experimental samples.

The basic equation for FN tunneling relates the tunneling current density to the applied electric field and is given below [22]

$$J = \frac{I}{A} = \frac{q^3 m}{8\pi h m_{ox} \phi_B} E^2 \exp\left(\frac{-8\pi/3qh(2m_{ox})^{1/2}\phi_B^{3/2}}{E}\right). \tag{2.30}$$

From (2.30) it can be seen that the electric field E across the oxide can be controlled by the tunneling current density J through the oxide. This is the principle behind constant current stressing, the technique used to high field stress devices in this thesis. Switching the polarity of the stressing current allows electrons to tunnel to or from the gate electrode.

If the stressing is allowed to continue for a long enough period of time, continued charge trapping in the oxide will raise the electric fields in the oxide to levels sufficient for dielectric breakdown. The amount of charge needed to tunnel through the oxide for this to occur is referred to as the charge-to-breakdown Q_{BD}. This parameter is often used in evaluating the reliability of an oxide [23]. Current levels during Q_{BD} testing are usually much higher than those used to generate interface traps so as to reduce the required stress time interval.

CHAPTER 3

EXPERIMENTAL DETAIL

N- and p-channel MOS transistors were subjected to high field stressing by means of a constant gate current. Periodically, the stressing was interrupted allowing the charge-pumping, subthreshold swing and $1/f$ noise methods for measuring D_{it} to be performed.

3.1 Experimental Devices

The transistors used in this thesis were fabricated by Sandia National Laboratories for the University of Arizona SEMATECH Center of Excellence for Contamination/Defect Assessment and Control. Six inch diameter wafers were processed in an abbreviated (no second metal or passivation) standard 1.25 μm twin-well CMOS process. Controlled levels of copper contamination were introduced to the buffered oxide etchant (BOE) used for the pre-gate oxidation clean. The gate oxide was then grown to a thickness of 180 Å. The surface doping levels are 1×10^{17} cm^{-3} for the n-channel transistors and 3×10^{16} cm^{-3} for the p-channel transistors. The n-channel devices have a lightly-doped drain structure while the p-channel devices do not.

The channel dimensions for the n- and p-channel transistors used in this thesis are the same; the width is 5 μm and the length is 20 μm. These particular dimensions provide

the best compromise between the requirements of the three methods. To avoid the geometric component in charge-pumping measurements, (W/L) should be as large as possible. For the equations used in the subthreshold swing method to be valid, L must be greater than or equal to 20 μm. And for the $1/f$ noise levels to be much higher than the background noise, the area ($W*L$) should be as small as possible. The transistors are from two lots processed with different amounts of copper contamination. Lot "L" had a copper concentration of 1 ppb while lot "H" had a concentration of 100 ppb. A detailed description of the process and devices is given in [24]. All the transistors tested were packaged in 40 pin ceramic dual-inline-packages (DIPs).

3.2 Experimental Technique

A HP4145B Semiconductor Parameter Analyzer was used to constant current stress the transistors. With the source, drain and substrate grounded, a current of either plus or minus 1 nA was forced into the gate. This translates to a current density of ±1 mA/cm^2. The measured electric field across the oxide during stressing was approximately 10 MV/cm. The devices were stressed for a total of 5000 s which corresponds to a fluence of 5 C/cm^2. This value is well below the charge-to-breakdown. With a current density of +10 mA/cm^2, Q_{BD} was found to be approximately 60 C/cm^2.

The stressing was interrupted periodically so that the D_{it} measurements could be performed. First, the subthreshold characteristics were determined with the HP4145B. Next the threshold voltage V_T was measured, again with the HP4145B, for use in the $1/f$ noise measurement. It was found that the linear method for measuring V_T provided the

best experimental fit to the number fluctuation model in (2.28). In this method, I_D is measured as a function of V_{GS} under a small fixed drain voltage bias. The drain current in this region is approximated by

$$I_D = \mu_n C_{ox}\left(\frac{W}{L}\right)\left[(V_{GS} - V_T)V_{DS} - \frac{V_{DS}^2}{2}\right]. \tag{3.1}$$

By extrapolating the linear portion of the I_D curve to $I_D = 0$ as illustrated in Figure 3.1, it is possible to estimate V_{GS0} and use this value to determine V_T using the following equation

$$V_T = V_{GS0} - \frac{V_{DS}}{2}. \tag{3.2}$$

The V_T measurements in this thesis were performed with V_{DS} equal to 100 mV.

After V_T was calculated, the $1/f$ noise was measured. The biasing conditions were the same for all measurements; the D.C. drain voltage V_{DS} was set equal to 200 mV and (V_{GS} - V_T) was set to 1 V. A frequency range of 2 - 250 Hz was used to calculate the $1/f$

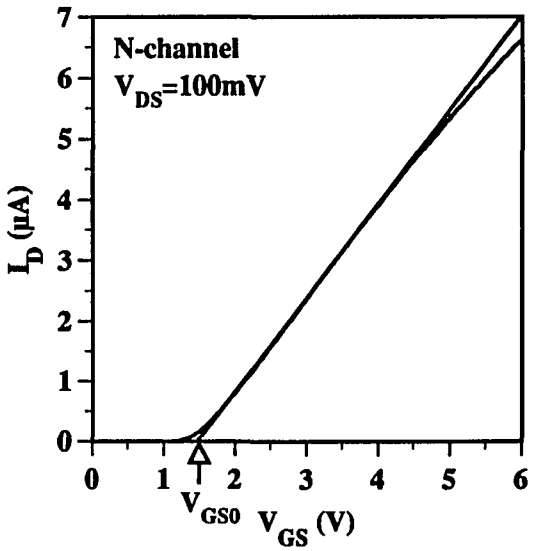

Figure 3.1 Plot of I_D versus V_{GS}. V_{GSO} is the extrapolated value of V_{GS} for $I_D = 0$ A. This value is used to determine V_T.

noise parameters in (2.28). Under these conditions, the $1/f$ noise of the transistors was significantly larger than the background noise as shown in Figure 3.2. Appendix A provides a detailed description of the actual system used to measure the $1/f$ noise.

Charge-pumping measurements were performed with an 8 $V_{p\text{-}p}$ triangle wave applied to the gate. The slope of the Q_{CP} versus $\ln(f)$ was found from a least squares fit to 10 data points. To verify that the charge-pumping was proceeding as predicted by (2.5), the correlation coefficient of the best fit line was calculated after each measurement. The coefficient was always greater than 0.97, indicating that there was no appreciable geometric component in the measured substrate current. Appendix B provides a more complete explanation of the charge-pumping measurement system.

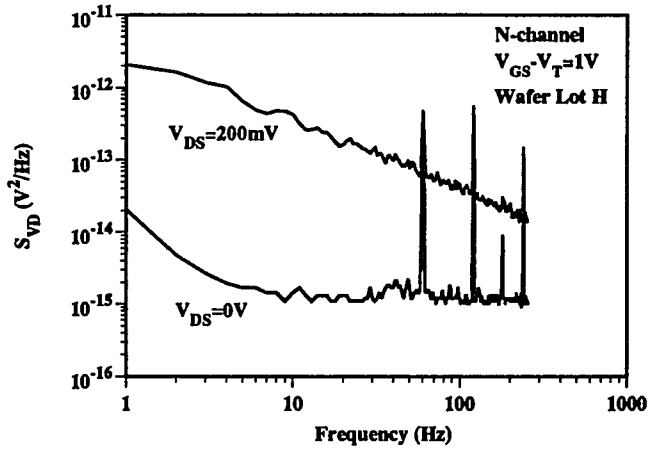

Figure 3.2 S_{V_D} versus f for V_{DS} = 200 mV and V_{DS} = 0 V with (V_{GS} - V_T) = 1 V. As can be seen, the noise level for V_{DS} = 200 mV is much greater than the background noise (V_{DS} = 0 V). The spikes in the plots are due to 60 Hz harmonic pickup. They are not included in the $1/f$ noise calculations. See Appendix A for a more detailed description of the $1/f$ noise measurement system.

CHAPTER 4

EXPERIMENTAL RESULTS

In this chapter, the experimental results of the three methods are presented. To provide a basis for comparison, three different groupings of transistors were tested under each method. These groupings were

Constant current stressing polarity (positive or negative)

Transistor wafer lot (L or H).

Transistor type (n- or p-channel).

For the charge-pumping and subthreshold swing methods, D_{it} is found to increase with stress time, independent of stressing polarity, wafer lot or transistor type. The results of the two methods yield reasonably close values of interface trap densities. The $1/f$ noise constant $K_{1/f}$ increases with stress time, independent of stressing polarity and wafer lot. However, by the end of the stressing, the noise constant in n-channel devices has increased several orders of magnitude more than the p-channel noise constant. A large discrepancy is then found between D_{it} in n-channel transistors calculated from the $1/f$ noise constant and charge-pumping/subthreshold measurements. The $1/f$ D_{it} results for p-channel transistors are in close agreement with the results of the other two methods.

Four transistors from each of the groupings listed above were measured during the experiment. Figure 4.1a shows a plot of the charge-pumping D_{it} results for a set of n-channel transistors stressed with a positive constant current. All four transistors exhibit

similar increases in the level of interface traps as a function of stress time. In Figure 4.1b, the devices from Figure 4.1a are normalized by the initial D_{it} values. Transistor #4 shows the largest normalized increase which may be a result of its initial D_{it} value being the lowest. In the following sections, the average value of the measurements performed on the transistors from each grouping is plotted. Error bars indicate the range of the measurements. For some plots, the range is so small that the error bars are difficult to see.

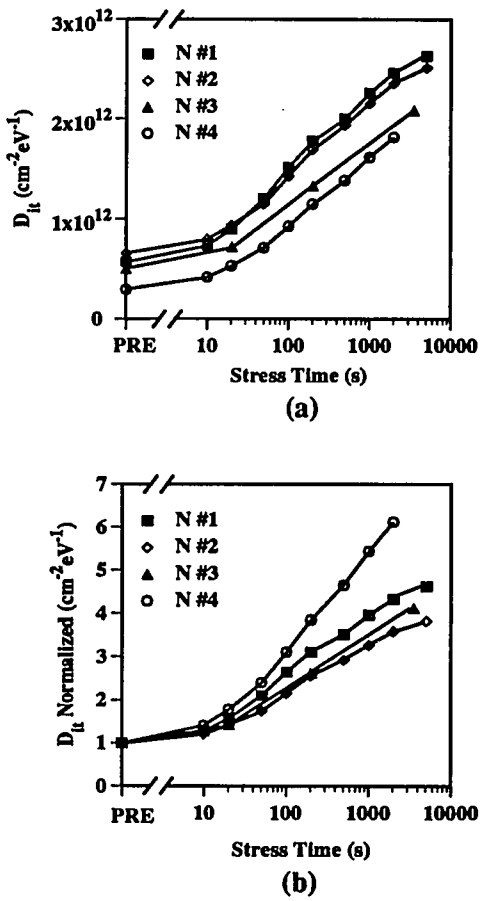

Figure 4.1 D_{it} as measured by the charge-pumping method for n-channel transistors. Measured values are shown in (a) and normalized by the initial value in (b).

4.1 Charge-Pumping

Figures 4.2, 4.3 and 4.4 show the results for the charge-pumping method. In Figure 4.2, the value of D_{it} as a function of stress time is compared for positive and negative stress currents. Figure 4.3 shows a comparison of D_{it} generation for the two different wafer lots. The results for n- and p-channel devices as measured by the charge-pumping method are given in Figure 4.4. The relatively large error bars in Figure 4.4 are due to a larger spread in initial D_{it} values. As can be observed in Figures 4.2 to 4.4, no dependency of interface trap density on current polarity, wafer lot or transistor type is observed

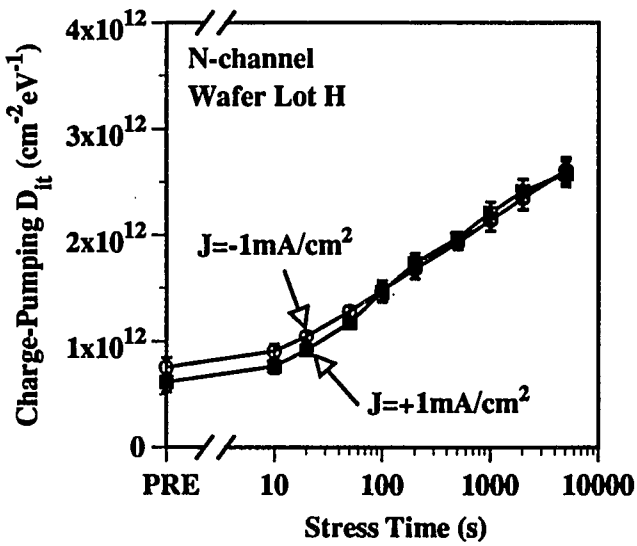

Figure 4.2 Charge-pumping D_{it} for positive and negative constant current stressing.

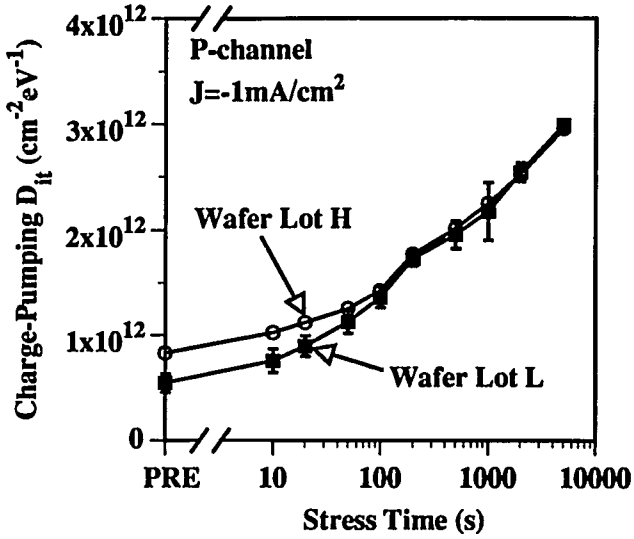

Figure 4.3 Charge-pumping D_{it} for devices from wafer lots L and H.

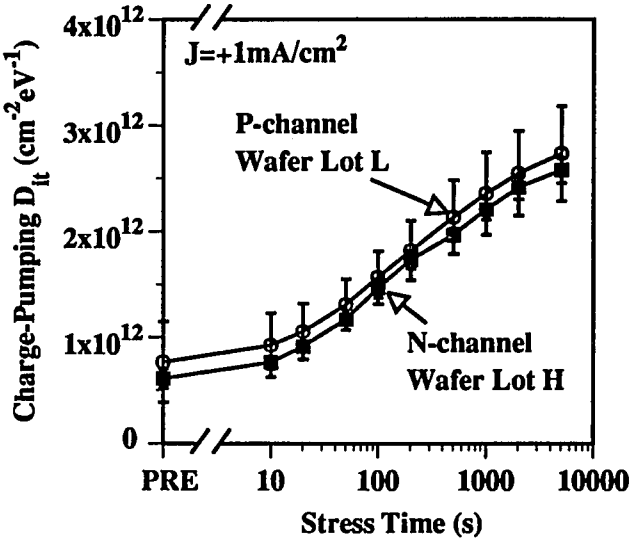

Figure 4.4 Charge-pumping D_{it} for n- and p-channel devices.

As described in Chapter 3, the transistors used in thesis originated from two lots processed with different buffered oxide etchants. These two lots were part of a 9 wafer set. A study of D_{it} values versus contamination level was performed using all 9 wafers [25]. The mean value of n-channel interface trap density (measured using the charge-pumping method) for each wafer is shown in Figure 4.5. The measurements were performed with an automated tester on 49 transistors per wafer. In the figure, the wafers are grouped by contamination levels: 0, 10 and 100 ppb. The devices used in this thesis were from wafers 12 and 15 as indicated. No obvious dependency of D_{it} on contamination level is seen in Figure 4.5. This agrees with the results shown in Figure 4.3 for high field stressed devices.

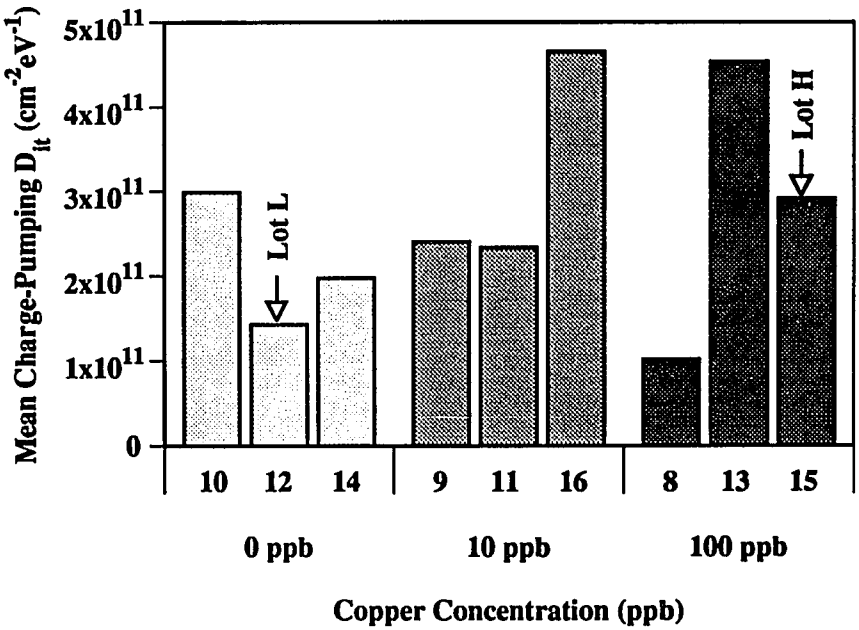

Figure 4.5 Mean charge-pumping D_{it} for wafers with different levels of copper contamination. The set of numbers closest to the x axis indicates the individual wafer numbers. The second set of numbers indicates the copper concentration in ppb.

4.2 Subthreshold Swing

The results of the subthreshold slope method appear in Figures 4.6 through 4.8. The actual subthreshold swing is plotted in these figures. In section 4.5 the value of D_{it} obtained by the subthreshold swing method is presented. Figure 4.6 illustrates the change in swing through constant current stressing for positive and negative currents. Devices from the two wafer lots are compared in Figure 4.7. In Figure 4.8, the results for n- and p-channel devices are given. Notice in Figure 4.8 that the swing for n-channel devices increases more than that of p-channel devices. The n-channel devices have a higher substrate doping level, which from (2.11) is seen to result in a higher swing S for a given interface trap density. Figures 4.6 and 4.7 show that the subthreshold swing is independent of current polarity, wafer lot and transistor type. In section 4.4.1, the difference in substrate doping levels between the n- and p-channel transistors is accounted for and it is shown that the D_{it} values calculated from subthreshold swing are independent of transistor type.

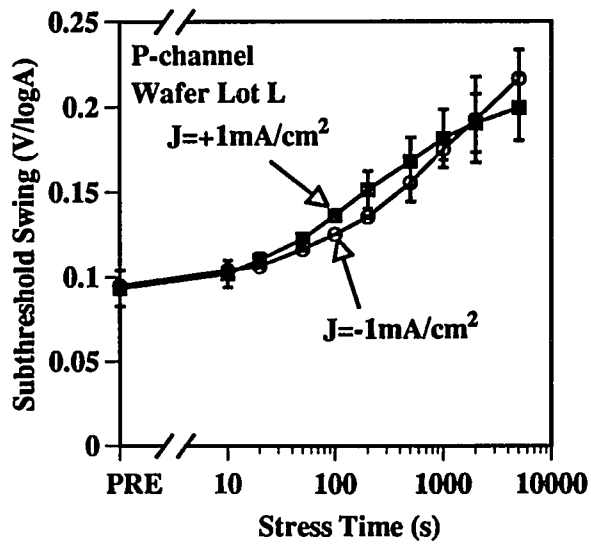

Figure 4.6 Subthreshold swing for positive and negative constant current stressing.

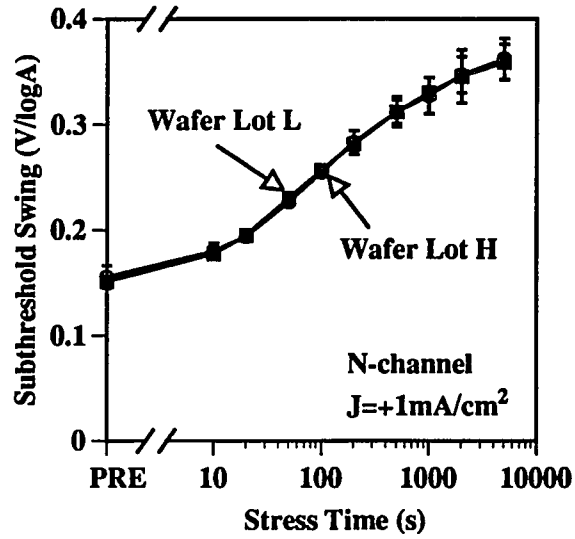

Figure 4.7 Subthreshold swing for devices from wafer lots L and H.

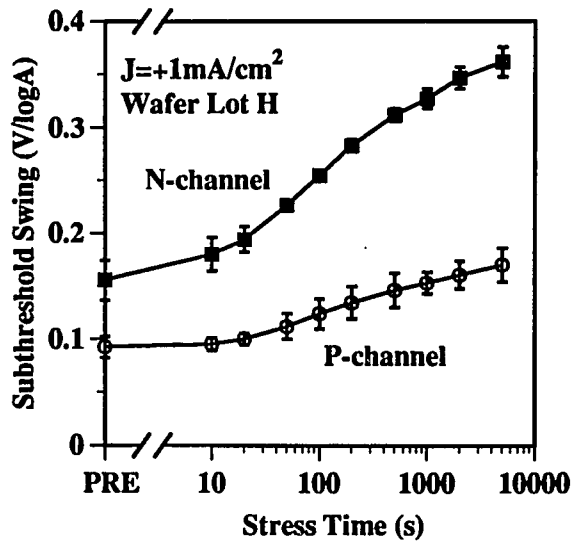

Figure 4.8 Subthreshold swing for n- and p-channel devices.

4.3 1/*f* Noise

The results of the third method, 1/*f* noise, are shown in Figures 4.9 through 4.12. After the noise measurements, the data were fit by the least squares method to the equation

$$S_{V_D} = \frac{A}{f^B} \tag{4.1}$$

where A is identical to the factor $\frac{V_{DS}^2}{(V_{GS}-V_T)^2} K_{1/f}$ in (2.28). For true "1/*f*" noise, B should be unity. Figure 4.9 shows B for n- and p-channel transistors during a typical measurement trial. For all the trials, B was close to unity. In Figures 4.10 to 4.12, the noise constant $K_{1/f}$ is plotted.

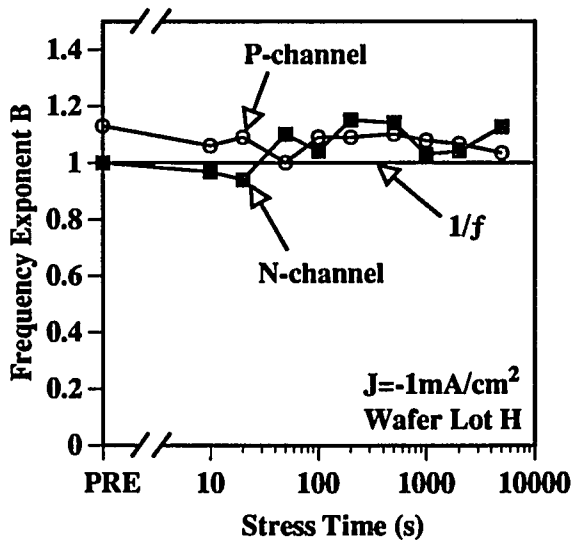

Figure 4.9 Frequency exponent of measured 1/*f* noise for n- and p-channel devices. The straight line indicates the frequency exponent of true "1/*f*" noise.

Figure 4.10 illustrates the noise development for positive and negative stress currents. There are no error bars on the negative stress data points (circles) as only one device was tested. Devices from wafer lots L and H are compared in Figure 4.11. And finally, the results for n- and p-channel transistors are displayed in Figure 4.12. At the higher stress levels, the noise in n-channel devices becomes very large. Some fluctuation is seen here and the noise constant $K_{1/f}$ occasionally decreases with further stressing. To highlight the general noise response as a function of stress time, a trend line is included in Figures 4.10 and 4.12.

From Figures 4.10 and 4.11, one sees that there appears to be no dependency on current polarity or wafer lot in the noise constant measurements. However, note the dramatic difference as shown in Figure 4.12 for the noise constant in n- and p-channel devices. Unlike in the subthreshold swing case, this difference can not be explained by the difference in substrate doping levels as $1/f$ noise in not dependent on that parameter.

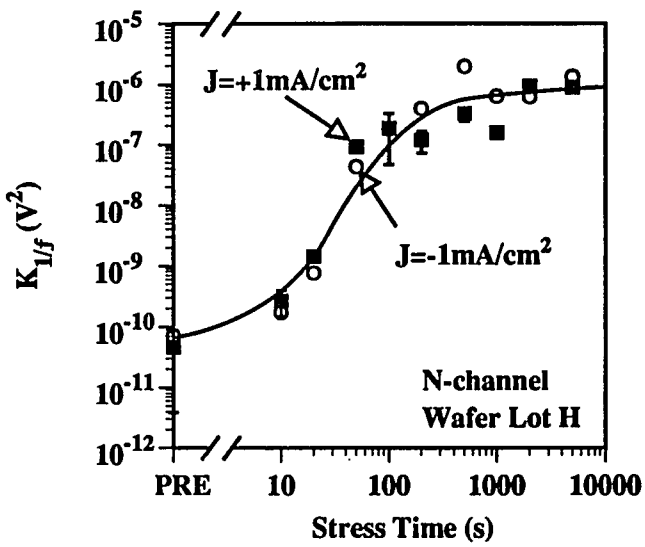

Figure 4.10 $1/f$ noise constant for positive and negative constant current stressing.

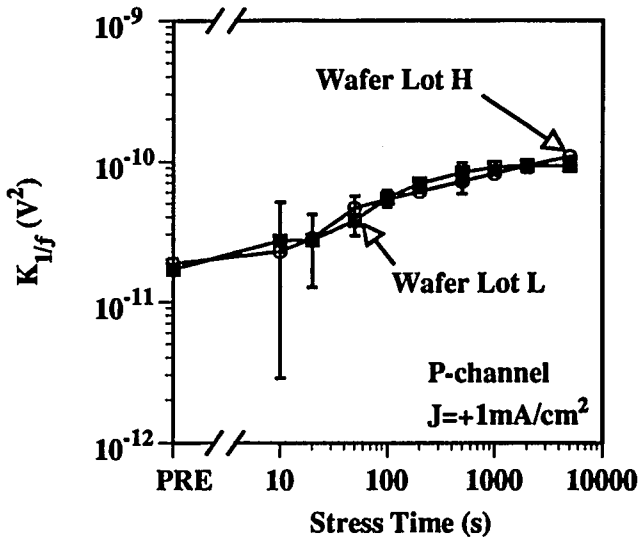

Figure 4.11 1/*f* noise constant for devices from wafer lots L and H.

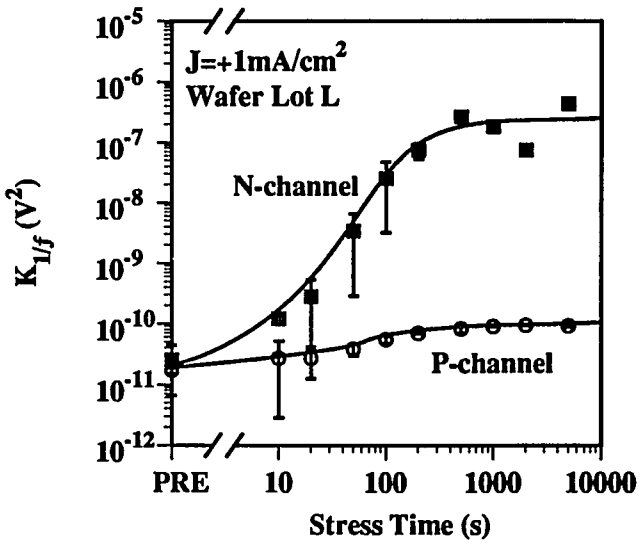

Figure 4.12 1/*f* noise constant for n- and p-channel devices.

4.4 Comparison Between Methods

4.4.1 Subthreshold Swing versus Charge-Pumping

The subthreshold swing values are used in (2.12) to calculate D_{it}, which is then plotted versus the results of the charge-pumping measurements for a n-channel device in Figure 4.13. As seen from (2.5) and (2.12), there are no "free" parameters in the equations used to calculate D_{it} from the experimental results. A one-to-one correlation line is included on the plot. To compare the methods on p-channel devices, the more complicated equation (2.9) had to be used because the approximation $a \gg (C_D / C_{ox})$ used in deriving (2.12) was no longer true. Using (2.9), the interface trap density from the subthreshold swing method is determined and plotted versus charge-pumping values in Figure 4.14. The two methods yield reasonably close values of D_{it} through the stressing for both n- and p-channel transistors.

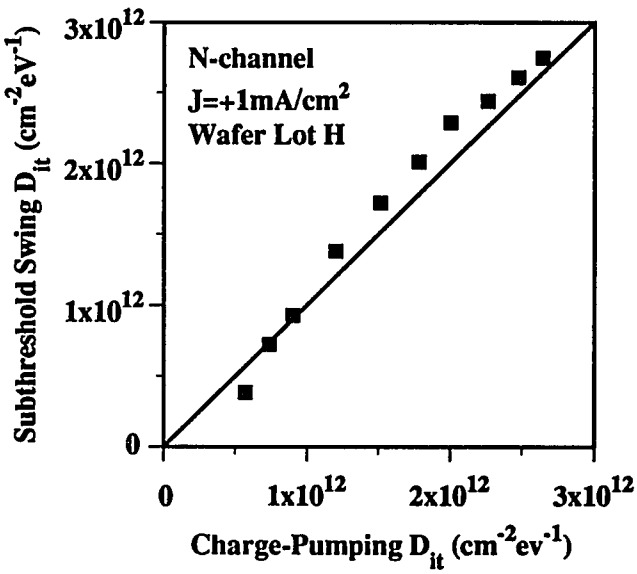

Figure 4.13 Comparison of D_{it} values from subthreshold swing and charge-pumping methods for a n-channel device.

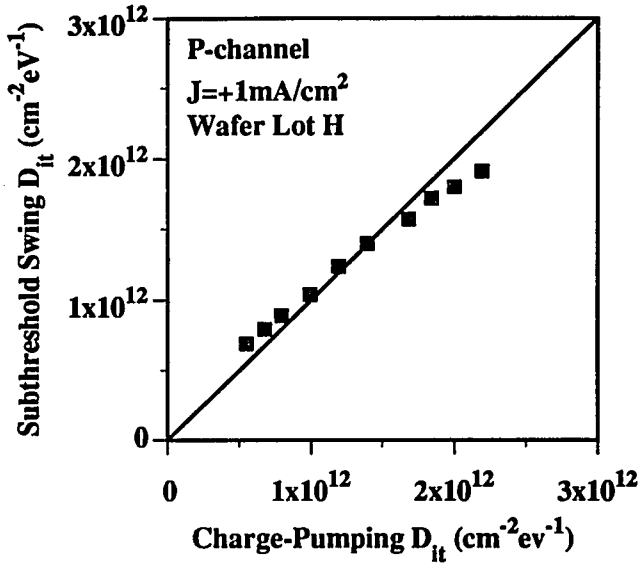

Figure 4.14 Comparison of D_{it} values from subthreshold swing and charge-pumping methods for a p-channel device.

4.4.2 1/*f* Noise versus Charge-Pumping/Subthreshold Swing

Using (2.29), D_{it} calculated from the 1/*f* noise measurements is plotted versus the values calculated with the charge-pumping method in Figure 4.15 and Figure 4.16. The only value somewhat "free" in determining D_{it} from the noise constant $K_{1/f}$ is the maximum tunneling distance d_t. As described in section 2.3, a value of 10 Å was used. Since the subthreshold swing values are in close agreement with the charge-pumping values as discussed in section 4.4.1, they are not directly compared with 1/*f* noise results.

As seen in Figure 4.15, there is obviously not a one-to-one correlation between the methods for n-channel devices. The n-channel D_{it} calculated from 1/*f* noise measurements increases by 5 orders of magnitude, while charge-pumping values of interface trap density increases by less than 1 order of magnitude. The results for p-channel devices are in better agreement. As seen in Figure 4.16, the two methods yield reasonably close values.

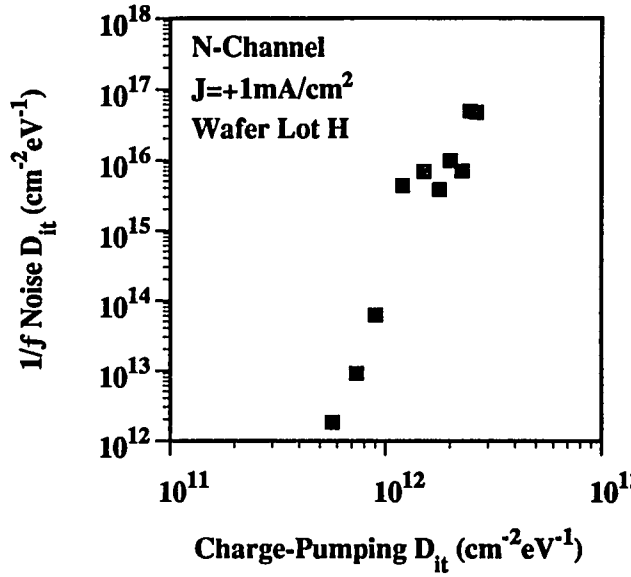

Figure 4.15 Comparison of D_{it} values from $1/f$ noise and charge-pumping methods for a n-channel device.

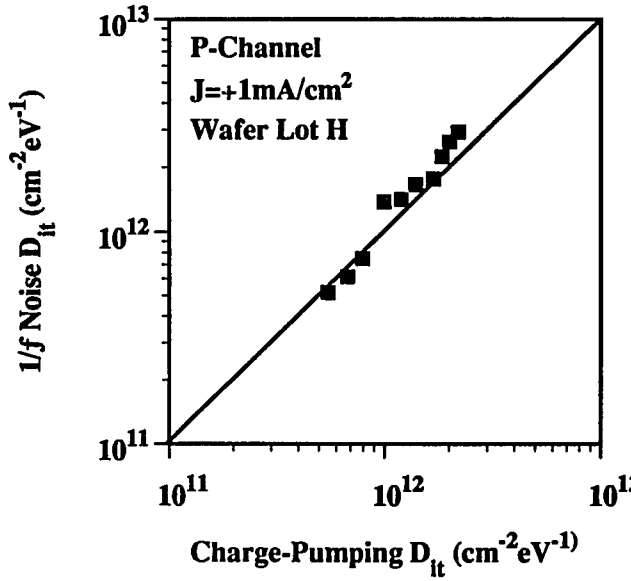

Figure 4.16 Comparison of D_{it} values from $1/f$ noise and charge-pumping methods for a p-channel device.

CHAPTER 5

SUMMARY AND CONCLUSIONS

This chapter summarizes the comparison of the three methods of measuring interface traps. The values for D_{it} obtained from charge-pumping and subthreshold swing methods are in close agreement. However, there is a very large difference in values produced by the $1/f$ noise method and the charge-pumping/subthreshold swing methods for n-channel transistors. The $1/f$ noise D_{it} results for p-channel transistors do agree quite well with the results of the other two methods.

5.1 Summary

The effects of high field stressing on the interface trap density in MOS transistors are compared using three measurement methods. These three methods, charge-pumping, subthreshold swing and $1/f$ noise, use different aspects of the interface traps in determining the trap density. As a result, each method measures interface trap density in different energy ranges within the bandgap. The n- and p-channel transistors were subjected to high field stress via constant current stressing to the gate. The stressing was periodically interrupted and all three measurements performed. The transistors originated from two wafer lots processed with different amounts of copper contamination in the buffered oxide etchant used for the pre-gate oxidation clean.

One of the motivations for this work was to investigate the effects of copper contamination on interface trap density. For all three methods, no dependency is found on contamination levels. The charge-pumping and subthreshold swing methods show no dependency on the polarity of the constant current applied to the gate or the transistor type (n- or p-channel). D_{it} calculated from these two methods are in close agreement.

As with the first two methods, no dependency is found on stress current polarity or wafer lot using the $1/f$ noise method. However, the results for the n- and p-channel comparison are quite different. After stressing to a fluence of 5 C/cm^2, the noise in the n-channel devices increased by several orders of magnitude while the noise in p-channel devices increased approximately one order of magnitude. The D_{it} values for n-channel devices calculated using the number fluctuation model for $1/f$ noise do not agree with the values derived from the charge-pumping/subthreshold swing methods. For the p-channel devices, a much better agreement is found between the three methods.

5.2 Conclusions

For transistors subjected to high field stress, the charge-pumping, subthreshold and $1/f$ noise (on p-channel devices) methods indicate a steady increase in the interface trap density. This trend has been reported by several authors [21,26,27]. In a similar study, Witczak et al. [28] have compared the charge-pumping and subthreshold swing methods, along with three capacitor-based methods, for MOS transistors exposed to gamma radiation. Their findings also show a good correlation between the charge-pumping and subthreshold swing methods.

As shown in Chapter 4, the results of the $1/f$ noise measurements on n-channel transistors do not correlate well with the other two methods. Also, the noise in the n-channel devices increased much more than that of the p-channel devices. Early reports by Klassen [29] and Broux et al. [30] describe a linear relationship between the noise and the interface trap density. However, their measurements were made on p-channel transistors biased in the saturated region; the measurements in this thesis were made in the linear region. Also, they referred the noise to the gate as opposed to the drain as done in this thesis. Some support and possible explanations for the discrepancy between noise response for n- and p-channel transistors and between the n-channel transistor $1/f$ noise results and the results of the other two methods follow.

Meisenheimer and Fleetwood have recently studied $1/f$ noise in MOS transistors subjected to ionizing radiation [31,32]. For their experiments, they biased the transistors in the linear region and measured the drain noise S_{V_D}. Two of their findings are of particular interest. First, for n-channel transistors subjected to ionizing radiation and subsequent anneal, they found a correlation between $1/f$ noise and oxide trapped charge, not interface traps. In their experiment, $1/f$ noise, D_{it} and oxide-trapped charge were monitored through irradiation and anneal. During irradiation all three of the previously mentioned values increased, but during the positive bias anneal, $1/f$ noise and oxide-trapped charge decreased while the interface trap density remained approximately the same. Second, they reported a different response in $1/f$ noise to post-irradiation anneal for n- and p-channel devices. The noise in n-channel transistors appears to be proportional to oxide-trapped charge whereas the noise in p-channel transistors behaves quite differently, almost inversely proportional to oxide-trapped charge.

In studying $1/f$ noise in irradiated power MOSFETs, a similar difference between n- and p-channel device noise response has been found [33]. P-channel power MOSFETs show a linear dependence on interface trap density through irradiation and anneal. N-channel power MOSFETs, however, show a linear dependence on oxide trap charge as reported for IC MOS transistors [32].

In deriving the number fluctuation model for $1/f$ noise in Chapter 2, the density of traps N_t is used. This is the number of traps per unit volume per unit energy. To compute the interface trap density, this value is multiplied by the maximum tunneling distance d_t. All traps located within this region are assumed to contribute to the $1/f$ noise. In the other two methods, charge-pumping and subthreshold slope, only those traps very close to the interface are measured [34]. Therefore, traps of a somewhat different nature are measured by the $1/f$ noise method as compared to those measured by the other two methods.

During constant current stressing, charge becomes trapped in the oxide resulting in a shift in threshold voltage. If the charge buildup is not uniform, it is possible that the simple MOS transistor theory used in deriving the equations in Chapter 2 is not valid. For this to explain the difference between n- and p-channel devices, the charge buildup would have to affect only the n-channel devices. The n-channel devices do have a LDD structure which could account for a different susceptibility to the charge buildup.

APPENDIX A

1/f NOISE MEASUREMENT SYSTEM

A block diagram of the $1/f$ noise measurement system used in this thesis is shown in Figure A.1. The device under test (D.U.T.) is placed inside the shielded bias circuit and the biasing resistor R_D is inserted into a special socket on the circuit board of the bias circuit. The value of R_D used in this thesis was 500 KΩ, much greater than the channel resistance $\left(\frac{1}{g_D}\right)$. After inserting R_D, V_{GS} and V_{DS} are set to the desired values. The output of the bias circuit is then A.C. coupled to a low-noise amplifier which in turn is connected to a spectrum analyzer. The averaged data from the spectrum analyzer are transferred to a computer over a GPIB (general purpose interface bus) connection. After the data transfer, the computer calculates the drain-source spectral density S_{V_D} and performs a linear regression computation to determine the best fit parameters A and B where

$$S_{V_D} = \frac{A}{f^B} \tag{A.1}$$

A plotter and printer connected to the computer allow hardcopies of the data. Also, the data can be saved to disk and later transferred to IBM compatible machines using the program LIF UTILITIES from Hewlett Packard. A more detailed description of each of the blocks follows below.

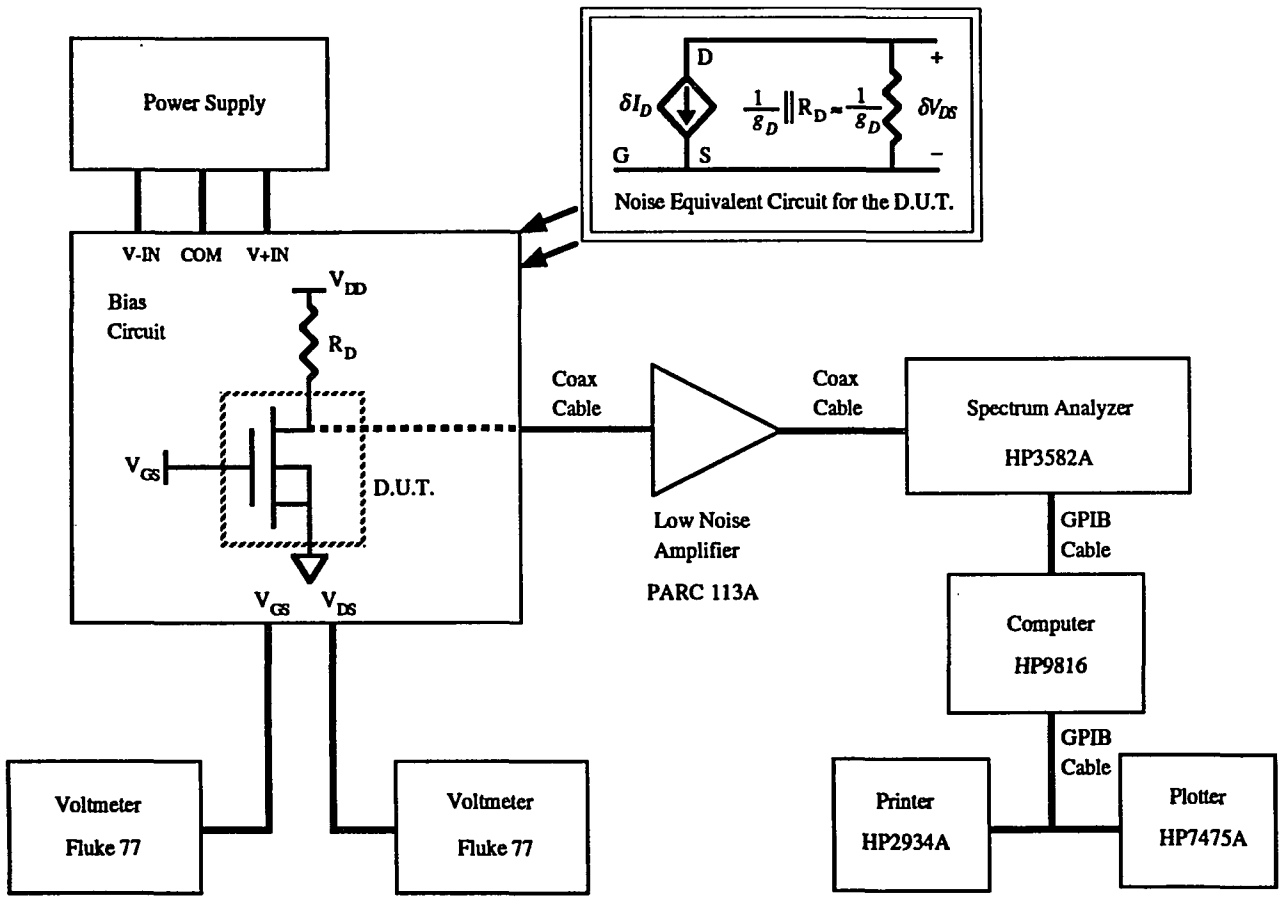

Figure A.1 1/*f* noise measurement system block diagram.

Bias Circuit:

The low-noise biasing circuit designed for the measurement system is shown in Figure A.2. Two Analog Devices 587 voltage references each coupled with two RC low-pass filters provide extremely low noise references which are buffered and inverted by OP27 op amps. Two 5 KΩ 10-turn wirewound potentiometers are used to adjust V_{GS} and V_{DD} between -10 V to 10 V (a jumper must be set on the circuit board depending on the device type, n- or p-channel, to select the correct polarity for V_{DD}). Four output transistors provide the current source for the D.U.T.

Low-pass filters inserted in the power lines reduce 60 Hz harmonic pickup. These filters have large time constants and the bias circuit, when initially powered, must be given a few minutes to stabilize before using. For the AD587 references to work properly, V+ must be a few volts larger than +10 V and V- a few volts less than -10 V. To compensate for IR drops in the low-pass filters, V+ IN and V- IN should be set to +18 V and -18 V, respectively.

Power Supply:

Figure A.3 shows the schematic for the power supply. The outputs are short-circuit protected with a maximum output current of approximately 500 mA. As in the bias circuit, low-pass filters reduce 60 Hz harmonic pickup.

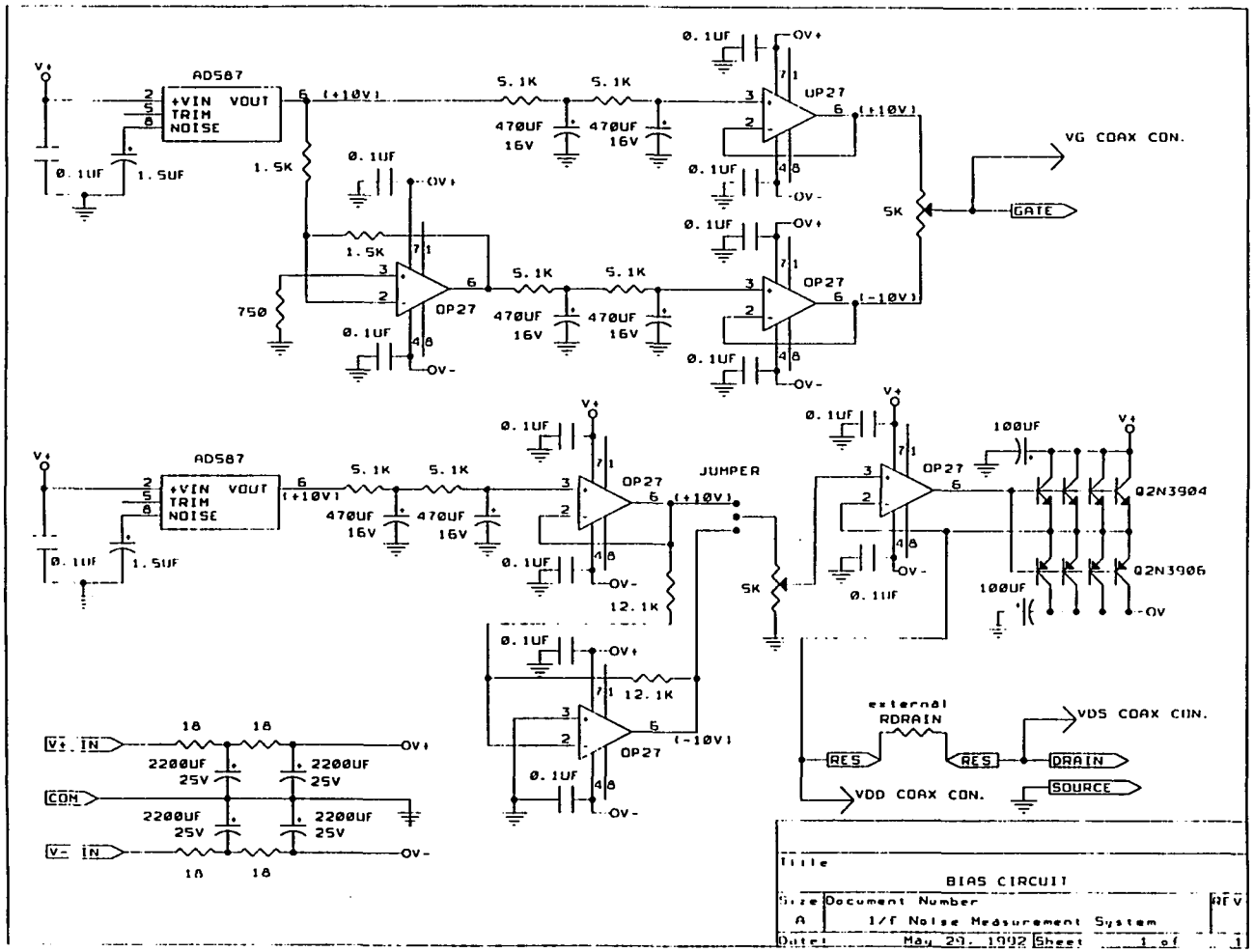

Figure A.2 Bias Circuit Schematic.

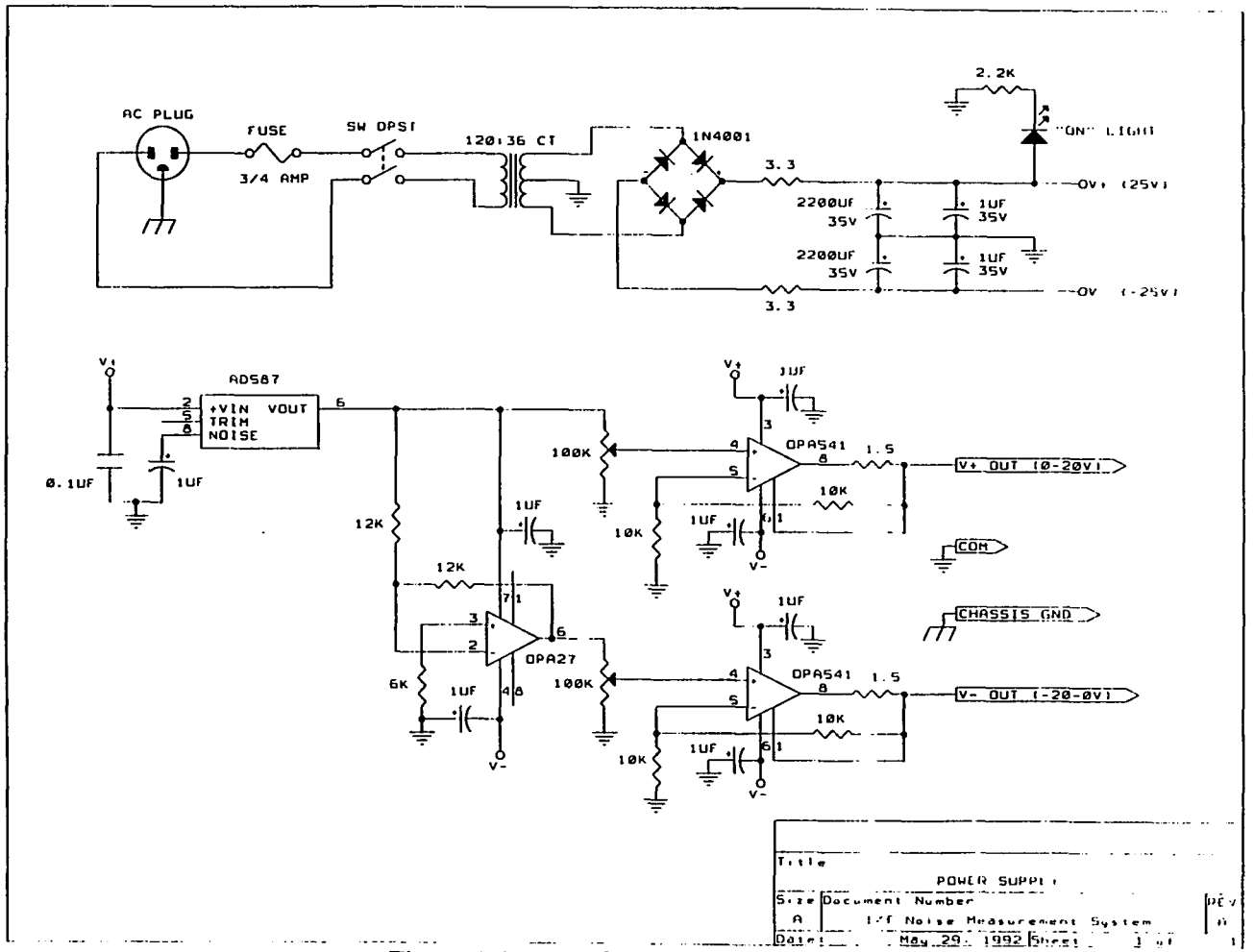

Figure A.3 Power Supply Schematic.

Low-Noise Amplifier:

A PARC 113 low-noise amplifier magnifies the drain-source voltage fluctuations from the D.U.T. to levels more suitable for the spectrum analyzer. For the measurements in this thesis, the gain of the amplifier was set to 5000 and the amplifier's low-pass and high-pass corners were set to 0.3 Hz and 3.0 kHz, respectively. To reduce 60 Hz pickup, the amplifier was unplugged from the A.C. outlet and powered by internal batteries during measurements.

Spectrum Analyzer:

An HP3582A spectrum analyzer converts the time-domain drain-source voltage fluctuations to frequency-domain data. In this thesis, each $1/f$ noise measurement was RMS averaged 128 times using a Hanning window. The frequency span of the analyzer was set to 250 Hz and the channel sensitivity was adjusted for maximum resolution.

Computer:

The HP Basic 3.0 program run on the HP9816 computer is listed in Figure A.4. The program accomplishes four separate tasks. First, the computer program controls the transfer of data from the spectrum analyzer. Second, the software computes S_{V_D}, incorporating the low-noise amplifier's gain and the spectrum analyzer's bandwidth into the calculation. If needed, the background noise, previously stored on disk, can be subtracted from the measured S_{V_D} values. No background noise subtraction was necessary for the devices used in this thesis as their noise levels were much larger than the background noise. Third, the best fit parameters are calculated using linear regression. Finally, the program prompts the user to print or plot hardcopies of the data or to save the data to disk.

```
10    !*************************************************************************
20    !*************************************************************************
30    !**                                                                     **
40    !**      FNOISE                                                         **
50    !**                                                                     **
60    !**      HP Basic 3.0 program for HP9816 computers                      **
70    !**      Calculates 1/f noise in MOSFETS from data extracted            **
80    !**      from an HP 3582A spectrum analyzer - GPIB Address: 711         **
90    !**                                                                     **
100   !*************************************************************************
110   !*************************************************************************
120   !*                                                                       *
130   !*                    Variable Definitions                               *
140   !*                                                                       *
150   !*      A,B ------- Best fit parameters: Sv = A/f^B                      *
160   !*      A$,B$ ----- Best fit parameter strings for disk storage          *
170   !*      Bkgnd(*) -- Background noise                                     *
180   !*      Cls$ ------ Clear screen string                                  *
190   !*      Com$ ------ Comment string for data storage to disk              *
200   !*      Erms(*) --- Spectrum analyzer data array                         *
210   !*      F(*) ------ Frequency value array                                *
220   !*      Fbw ------- Frequency analzyer bandwidth                         *
230   !*      Fspan ----- Frequency span setting of spec. anal.                *
240   !*      Gain/Gain$- Gain/gain string  of preamplifier                    *
250   !*      Mtitles$ -- Menu title string used by Menu1                      *
260   !*      Numpts ---- Number of freq samples used by program               *
270   !*      Ptype ----- Flag to specify output to screen or hardcopy         *
280   !*      R --------- Correlation coefficient of best fit                   *
290   !*      Sv(*) ----- Noise data array                                     *
300   !*      T$ -------- Title string used by output subprograms              *
310   !*      X$/Y$ ----- X/Y axis label string                                *
320   !*                                                                       *
330   !*************************************************************************
340   !
350   OPTION BASE 1                              !Array indexes start @ 1
360   DIM F(19),Sv(19),Erms(19),Bkgnd(19)
370   DIM X$[20],Y$[30],A$[25],B$[25],Com$[36],Quit$[36]
380   DIM Dtitle$[35],Mtitle$[55]
390   Cls$=CHR$(255)&"K"                         !Clear screen string
400   ON ERROR GOTO Eroutine                     !Disk error handling routine
410   GOSUB Startscreen                          !Optional info screen rountine
420   GOSUB Datapts                              !Subrtn where freq samples chosen
430 Start: !
440   GOSUB Dataretrieve                         !Retrieve data from spectrum anlz.
450   GOSUB Input                                !Input user data
460   GOSUB Noise                                !Calculate SV
470   GOSUB Bestfit
480   Mtitle$="Svd Data Calculated from Spectrum Analyzer Data"
490   GOSUB Menu1
500   GOTO Start                                 !Loop back to rerun program
510   !
520   !*************************************************************************
530   !                Startup Screen Subroutine
540   !  Displays necessary setup conditions to run program
550   !*************************************************************************
560 Startscreen:  !
570   OUTPUT 2 USING "#,K";Cls$                       !Clear screen
580   PRINT ""
590   PRINT "   ... FNOISE ..."
600   PRINT ""
```

Figure A.4 Computer program for 1/*f* noise measurement system.

```
610   PRINT "1/f noise extraction program for HP3582A Spectrum Analyzer"
620   INPUT "Do you want to see the Info Screen? (ret)=no",Answ$
630   Answ$=UPC$(Answ$)              !translate "Answ$" to all upper case
640   IF Answ$[1,1]="Y" THEN
650     PRINT "     This program uses data from an HP spectrum analyzer"
660     PRINT "to compute 1/f noise.  The data must be in the spectrum"
670     PRINT "analyzer's buffer before running this program.  Only a"
680     PRINT "sampling of the frequencies are used.  These values are"
690     PRINT "stored in the program's F(*) array.  To change the values"
700     PRINT "used you must edit the DATA line and NUMPTS variable."
710     PRINT ""
720     PRINT "     If you are going to save data make sure the data disk"
730     PRINT "is in drive "":,700,0"" Also, if you are going to be subtracting"
740     PRINT "the background noise from the measured data, be sure the back-"
750     PRINT "ground data is in a file named ""BKGND"""
760     PRINT ""
770     PRINT TAB(13),"Equipment",TAB(46),"GPIB Address"
780     PRINT TAB(10),"HP7475A Plotter",TAB(50),"05"
790     PRINT TAB(10),"HP2934A Printer",TAB(50),"01"
800     PRINT TAB(10),"HP3582 Spectrum Analyzer",TAB(50),"11"
810     PRINT ""
820     PRINT "Hit ""Continue"" key when ready"
830     PAUSE
840   END IF
850   Answ$=""
860   RETURN
870   !
880   !*************************************************************************
890   !               Data Point Selection Subroutine
900   !  The frequency points to be used in 1/f calculations are set in
910   !  this subroutine.  If a different number of points are used,
920   !  NUMPTS must be updated.
930   !  Returns value of SUMPTS
940   !*************************************************************************
950 Datapts:  !
960   DATA 2,3,4,5,6,7,8,9,10,20,30,40,50,70,80,90,100,200,250
970   Numpts=19                                 !Number of points in DATA line
980   FOR I=1 TO Numpts
990     READ Pt
1000    F(I)=Pt                                 !load array F(*) with data
1010  NEXT I
1020  RESTORE 960
1030  RETURN
1040  !
1050  !*************************************************************************
1060  !               Data Retrieve Subroutine
1070  !  Retrieves data from HP spectrum analyzer 3582A
1080  !  Assumes GPIB address of spec. anal. is 711
1090  !  Uses marker value (MP) instead of LDS for improved accuracy
1100  !  Returns values of FSPAN, ERMS(*) to main program
1110  !*************************************************************************
1120 Dataretrieve: !
1130  PRINT ""
1140  PRINT "Hit ""Continue"" to start retrieving data from spectrum analyzer"
1150  PAUSE
1160  PRINT ""
1170  PRINT "*************************************************"
1180  PRINT "***                                           ***"
1190  PRINT "***  retrieving data from HP spectrum analyzer  ***"
1200  PRINT "***                                           ***"
1210  PRINT "*************************************************"
```

Figure A.4 (continued)

```
1220  REMOTE 711
1230  OUTPUT 711;"LSP"                !Request Fspan from spec analz
1240  ENTER 711;Fspan
1250  IF Fspan<>250 THEN
1260    PRINT ""
1270    PRINT "Incorrect frequency span setting on spectrum analyzer!!!"
1280    PRINT "Set FSPAN=250 then redue measurement,"
1290    GOTO Dataretrieve
1300  END IF
1310  OUTPUT 711;"MN1"                !Turn marker on
1320  OUTPUT 711;"sc1"                !Set linear scal
1330  M$="MP"                         !Create marker string
1340  FOR I=1 TO Numpts               !Data retrieve loop...
1350  I$=VAL$(F(I))
1360  Mp$=M$&I$
1370  OUTPUT 711;Mp$
1380  OUTPUT 711;"LMK"                !Request marker value
1390  ENTER 711;Erms(I)
1400  NEXT I
1410  LOCAL 711
1420  BEEP
1430  RESTORE                         !Resets data pointer
1440  RETURN
1450  !
1460  !*************************************************************************
1470  !                    Input User Data Subroutine
1480  !  Prompts user for spectrum analyzer settings and biasings conditions
1490  !  Returns GAIN, & FBW to main program
1500  !*************************************************************************
1510 Input: !
1520  OUTPUT 2 USING "#,K";Cls$
1530  Gain=5000                                 !Pre amp gain
1540  Fbw=1.5                                   !Frequency bandwidth
1550  PRINT "Default setting is:"
1560  PRINT "preamp gain=5000"
1570  INPUT "Do you wish to change this? <ret>=no",Answ$
1580  Answ$=UPC$(Answ$)                         !Convert to uppercase
1590  IF Answ$[1,1]="Y" THEN
1600    Answ1$=""                               !Reset Input variable
1610    OUTPUT 2 USING "#,K";Cls$
1620    INPUT "Enter gain of preamplifier (ex. 2K, 5K etc.)",Gain
1630    PRINT "Preamp gain=",Gain
1640    INPUT "Is this value correct? <ret=no>",Answ1$
1650    Answ1$=UPC$(Answ1$)
1660    IF Answ1$[1,1]<>"Y" THEN GOTO 1610
1670  END IF
1680  Answ$=""
1690  Answ1$=""
1700  Gain$="gain = "&VAL$(Gain)                !Gain string used in plots
1710  RETURN
1720  !
1730  !*************************************************************************
1740  !                    Noise Subroutine
1750  !  Calculates noise of MOS from spectrum analyzer data and
1760  !  preamp gain
1770  !  Returns values of SV(*) array to main program
1780  !*************************************************************************
1790 Noise: !
1800  PRINT ""
1810  INPUT "Do you wish to subtract the background noise? <ret=no>",Answ$
1820  Answ$=UPC$(Answ$)
1830  PRINT ""
```

Figure A.4 (continued)

```
1840  IF Answ$[1,1]="Y" THEN
1850    Bkflag=1
1860    MASS STORAGE IS ":,700,0"              !Specify disk drive
1870    ASSIGN @Path TO "BKGND"                !Open I/O path
1880    PRINT ""
1890    PRINT "Reading ""BKGND"" file..."
1900    FOR I=1 TO Numpts                      !Retrieve data from disk...
1910      ENTER @Path;Scrap                    !Store freq value in temp var
1920      ENTER @Path;Bkgnd(I)
1930    NEXT I
1940    ASSIGN @Path TO *                      !Close I/O path
1950  ELSE
1960    Bkflag=0
1970  END IF
1980    Answ$=""
1990  PRINT "Calculating Svd..."
2000  PRINT ""
2010  FOR I=1 TO Numpts                        !Calculate SV...
2020    Sv(I)=(Erms(I)/Gain)^2/Fbw
2030  NEXT I
2040  IF Bkflag=1 THEN
2050    FOR I=1 TO Numpts
2060      Sv(I)=ABS(Sv(I)-Bkgnd(I))
2070    NEXT I
2080  END IF
2090  RETURN
2100  !
2110  !*************************************************************************
2120  !                    Best Fit Subroutine
2130  !  Uses simple linear regression by taking log of both sides of
2140  !  eqn:  Sv = A / (f)^B  resulting in LGT(Svg) = -B*LGT(f) + LGT(A)
2150  !  This is equivalent to y=mx+b with B=-m & A=10^c
2160  !  Returns values of A, B, R to main program
2170  !*************************************************************************
2180 Bestfit: !
2190  PRINT "Calculating Best Fit..."
2200  PRINT ""
2210  !Clear variables in case program is re-run
2220  Xsum=0                                   !Sum of x values
2230  Ysum=0                                   !Sum of y values
2240  Xbar=0                                   !Average of x values
2250  Ybar=0                                   !Average of y values
2260                                           !Delta x = (xi-xbar)
2270  Ssxx=0                                   !Sum of squares of delta x
2280  Ssyy=0                                   !Sum of squares of delta y
2290  Ssxy=0                                   !Sum of (delta x) * (delta y)
2300  FOR I=1 TO Numpts
2310    Xsum=Xsum+LGT(F(I))                    !Sum log of freq
2320    Ysum=Ysum+LGT(Sv(I))                   !Sum log of Svg
2330  NEXT I
2340  Xbar=Xsum/Numpts                             !Calculate xbar
2350  Ybar=Ysum/Numpts                             !Calculate ybar
2360  FOR I=1 TO Numpts
2370    Ssxx=Ssxx+(LGT(F(I))-Xbar)^2               !Calculate Ssxx
2380    Ssyy=Ssyy+(LGT(Sv(I))-Ybar)^2              !Calculate Ssyy
2390    Ssxy=Ssxy+((LGT(F(I))-Xbar)*(LGT(Sv(I))-Ybar)) !Cal. Ssxy
2400  NEXT I
2410  M=Ssxy/Ssxx                                  !Calculate M
2420  C=Ybar-M*Xbar                                !Calculate C
2430  A=10^C                                       !Calculate A
2440  B=-M                                         !Calculate b
2450  R=Ssxy/SQR(Ssxx*Ssyy)                        !Calculate coeff of corr.
2460  RETURN
2470  !
```

Figure A.4 (continued)

```
2480  !*************************************************************************
2490  !              Output Selection Menu Subroutine
2500  !  Prompts user for desired output format then calls appropriate
2510  !  subprograms
2520  !*************************************************************************
2530 Menu1: !
2540  OUTPUT 2 USING "#,K";Cls$
2550  Choice$=""
2560  PRINT ""
2570  PRINT Mtitle$
2580  PRINT ""
2590  PRINT "Select operation desired:"
2600  PRINT ""
2610  PRINT "A) PLOT to screen"
2620  PRINT "B) PLOT hardcopy"
2630  PRINT "C) PRINT to screen"
2640  PRINT "D) PRINT hardcopy"
2650  PRINT "E) SAVE to disk"
2660  PRINT "F) RERUN program"
2670  PRINT ""
2680  PRINT "X) EXIT"
2690  INPUT Choice$
2700  Choice$=UPC$(Choice$)                    !Convert to Uppercase
2710  SELECT Choice$
2720  CASE "A"
2730    Ptype=1                                !Flag to plot to CRT
2740    CALL Plot(Numpts,F(*),Sv(*),Ptype,A,B)
2750    GOTO Menu1
2760  CASE "B"
2770    Ptype=2                                !Flag to plot to plotter
2780    CALL Plot(Numpts,F(*),Sv(*),Ptype,A,B)
2790    GOTO Menu1
2800  CASE "C"
2810    Ptype=1                                !Flag to print to CRT
2820    CALL Print(Numpts,F(*),Sv(*),Ptype,A,B,R)
2830    GOTO Menu1
2840  CASE "D"
2850    Ptype=2                                !Flag to print to printer
2860    CALL Print(Numpts,F(*),Sv(*),Ptype,A,B,R)
2870    GOTO Menu1
2880  CASE "E"
2890    GOSUB Savedata
2900    GOTO Menu1
2910  CASE "F"
2920    RETURN
2930  CASE "X"
2940    GOTO End
2950  CASE ELSE
2960    GOTO Menu1
2970  END SELECT
2980  !
2990  !*************************************************************************
3000  !                    Save Data to Disk Subroutine
3010  !  Prompts user to save data to disk.  Saves data as ASCII file
3020  !  to MSI ":,700,0"
3030  !*************************************************************************
3040 Savedata: !
3050  OUTPUT 2 USING "#,K";Cls$                !Clear screen
3060  PRINT ""
3070  INPUT "Enter filename for data",Filename$
3080  Filename$=UPC$(Filename$)
```

Figure A.4 (continued)

```
3090  IF Filename$="BKGND" THEN
3100    PRINT ""
3110    PRINT "BKGND data will be saved to be later used by this program."
3120    PRINT "This data will be stored in a different format from that"
3130    PRINT "normally used."
3140    PRINT ""
3150    PRINT "Saving BKGND data..."
3160    MASS STORAGE IS ":,700,0"
3170    CREATE ASCII Filename$,5
3180    ASSIGN @Path TO Filename$
3190    FOR I=1 TO Numpts
3200      OUTPUT @Path;F(I)                    !Frequency value
3210      OUTPUT @Path;Sv(I)                   !Noise magnitude
3220    NEXT I
3230    ASSIGN @Path TO *
3240    RETURN
3250  END IF
3260  PRINT ""
3270  INPUT "Do you want to add comments? <ret=no>",Answ2$
3280  Answ2$=UPC$(Answ2$)
3290  MASS STORAGE IS ":,700,0"                  !Specify disk drive
3300  CREATE ASCII Filename$,5                   !Create file
3310  ASSIGN @Path_1 TO Filename$                !Open I/O path
3320  A$="!A = "&VAL$(A)                         !Best fit strings
3330  B$="!B = "&VAL$(B)                         !  "
3340  OUTPUT @Path_1;A$                          !Save best fit values
3350  OUTPUT @Path_1;B$                          !  "
3360  C$=","                                     !Data delimiter
3370  IF Answ2$[1,1]="Y" THEN
3380    PRINT ""
3390    PRINT "Enter comment lines one at a time, max 35 characters"
3400    PRINT "When finished, enter ""XXX"""
3410 Comments: !
3420    INPUT Com$
3430    Quit$=UPC$(Com$)
3440    IF Quit$<>"XXX" THEN
3450      Com$="!"&Com$                          !Add comment indicator
3460      OUTPUT @Path_1;Com$
3470      GOTO Comments                          !Loop back for more comments
3480    END IF
3490  END IF
3500  PRINT ""
3510  PRINT ""
3520  PRINT "saving Sv vs. Frequency data to file:",Filename$
3530  FOR I=1 TO Numpts                          !Store data to disk...
3540    OUTPUT String$ USING "#,DDD,A,DDD,A,D.DDDDE";F(I),C$,F(I),C$,Sv(I)
3550    OUTPUT @Path_1;String$
3560  NEXT I
3570  ASSIGN @Path_1 TO *                        !Close I/O path
3580  Answ$=""
3590  Answ2$=""
3600  RETURN
3610  !
3620  !*************************************************************************
3630  !                    Error Handling Subroutine
3640  !  This subroutine handles any disk errors that arise from either the
3650  !  NOISE or the SAVEDATA subroutines.
3660  !*************************************************************************
3670 Eroutine: !
3680  Enum=ERRN                                  !Determine error number
3690  PRINT ""
```

Figure A.4 (continued)

```
3700  PRINT ""
3710  PRINT "*******  ERROR OCCURRED  *******"
3720  PRINT ""
3730  SELECT Enum
3740  CASE 53
3750    PRINT "Improper file name"
3760  CASE 54
3770    PRINT "Duplicate file name"
3780  CASE 56
3790    PRINT "File name not found"
3800  CASE 58
3810    PRINT "Improper file type"
3820  CASE 64
3830    PRINT "Disk overflow"
3840  CASE 80
3850    PRINT "Disk not in drive"
3860  CASE 83
3870    PRINT "Disk write protected"
3880  CASE ELSE
3890    PRINT "Error number is:",Enum,ERRM$
3900  END SELECT
3910  PRINT ""
3920  PRINT "When the problem is corrected hit <Continue>"
3930  PAUSE
3940  IF ERRL(1870) THEN GOTO 1870     !Locate error line and return
3950  IF ERRL(1910) THEN GOTO 1910
3960  IF ERRL(1920) THEN GOTO 1920
3970  IF ERRL(1940) THEN GOTO 1940
3980  IF ERRL(3170) THEN GOTO 3170
3990  IF ERRL(3200) THEN GOTO 3200
4000  IF ERRL(3210) THEN GOTO 3210
4010  IF ERRL(3300) THEN GOTO 3300
4020  IF ERRL(3310) THEN GOTO 3310
4030  IF ERRL(3340) THEN GOTO 3340
4040  IF ERRL(3350) THEN GOTO 3350
4050  IF ERRL(3460) THEN GOTO 3460
4060  IF ERRL(3550) THEN GOTO 3550
4070  IF ERRL(3570) THEN GOTO 3570
4080  GOTO Eroutine
4090  !
4100 End: !
4110  PRINT ""
4120  PRINT "* * * * *    End of Program    * * * * *"
4130  END
4140  !
4150  !*************************************************************************
4160  !*                          Print Subprogram                             *
4170  !*************************************************************************
4180  SUB Print(Numpts,F(*),Sv(*),Ptype,A,B,R)
4190  DIM T$[50]
4200  Cls$=CHR$(255)&"K"                          !Clear CRT string
4210  OUTPUT 2 USING "#,K";Cls$                   !Clear CRT screen
4220  IF Ptype=2 THEN
4230    INPUT "Enter desired title heading (50 characters max)",T$
4240    INPUT "Print short listing? (no Sod vs. freq data) <ret=yes>",Lflag$
4250    Lflag$=UPC$(Lflag$)
4260    PRINTER IS 701
4270  END IF
4280  FOR I=1 TO 5
```

Figure A.4 (continued)

```
4290    PRINT ""
4300  NEXT I
4310  PRINT T$
4320  PRINT " "
4330  IF Lflag$[1,1]<>"N" THEN GOTO 4410
4340  PRINT "Equivalent Noise Power Spectral Density at the Drain:"
4350  PRINT " "
4360  PRINT "Freq(Hz)","      Svd"
4370  FOR I=1 TO Numpts
4380    PRINT F(I),Sv(I)
4390  NEXT I
4400  PRINT " "
4410  PRINT "Best Fit Data  Svd=A/(f)^b"
4420  PRINT " "
4430  PRINT "A =",A
4440  PRINT "b =",B
4450  PRINT " "
4460  PRINT "Correlation coefficient r =",R
4470  IF Ptype=1 THEN
4480    PRINT ""
4490    PRINT "Hit ""Continue"" when ready..."
4500    PAUSE
4510  END IF
4520  PRINTER IS 1
4530  Lst$=""
4540  SUBEND
4550  !
4560  !*************************************************************************
4570  !*                          Plot Subprogram                              *
4580  !*************************************************************************
4590  SUB Plot(Numpts,F(*),Sv(*),Ptype,A,B)
4600  DIM T$[34]
4610  Cls$=CHR$(255)&"K"                          !Clear screen variable
4620  OUTPUT 2 USING "#,K";Cls$                   !Clear CRT screen
4630  X$="Frequency (Hz)"                         !X axis label
4640  Y$="Svd (V^2/Hz)"                           !Y axis label
4650  INPUT "Do you want to include best fit line? <ret=yes>",Answ$
4660  Answ$=UPC$(Answ$)                           !Convert to uppercase
4670  IF Answ$[1,1]="N" THEN
4680    Bfflag=0
4690  ELSE
4700    Bfflag=1
4710  END IF
4720  Answ$=""
4730  !--- Calculate xmin,xmax,ymin,ymax by auto scaling ---
4740  Xmin=INT(LGT(F(1)))                         !Min expon of 10 for x
4750  Xmax=INT(LGT(F(Numpts)))                    !Max expon of 10 for x
4760  Diff=LGT(F(Numpts))-Xmax
4770  IF Diff>0 THEN Xmax=Xmax+1                  !Increment exp if needed
4780  INPUT "Do you want to enter y axis min & max values? <ret=no>",Answ$
4790  Answ$=UPC$(Answ$)
4800  IF Answ$[1,1]="Y" THEN
4810    Answ1$=""                                 !Reset Input variable
4820    OUTPUT 2 USING "#,K";Cls$
4830    PRINT "Enter only the exponent"
4840    PRINT "for example Ymin = ""-17"" (1E-17)"
4850    PRINT "for example Ymax = ""-14"" (1E-14)"
4860    PRINT ""
4870    INPUT "Enter Ymin,Ymax",Ymin,Ymax
4880    PRINT "Ymax =",Ymax
4890    PRINT "ymin =",Ymin
```

Figure A.4 (continued)

```
4900    INPUT "Are these correct? <ret=no>?",Answ1$
4910    Answ1$=UPC$(Answ1$)
4920    IF Answ1$[1,1]<>"Y" THEN GOTO 4820
4930    OUTPUT 2 USING "#,K";Cls$
4940  ELSE                                      !Auto scaling...
4950    Ymax=INT(LGT(Sv(1)))                    !Max expon of 10 for y
4960    Ymin=INT(LGT(Sv(Numpts)))               !Min expon of 10 for y
4970    Diff1=Ymax-LGT(Sv(Numpts))
4980    Diff2=Ymin-LGT(Sv(Numpts))
4990    IF Diff1>0 THEN Ymax=Ymax+1             !Increment exp if needed
5000    IF Diff2>0 THEN Ymin=Ymin-1             !Decrement exp if needed
5010  END IF
5020  Xrange=Xmax-Xmin
5030  Yrange=Ymax-Ymin
5040  Answ$=""
5050  Answ1$=""
5060  GINIT
5070  IF Ptype=2 THEN
5080    INPUT "Enter title of graph (max 34 characters)",T$
5090    PRINT "Make sure paper is in plotter, hit ""Continue"" when ready"
5100    PAUSE
5110    PLOTTER IS 705,"HPGL"
5120  ELSE
5130      PLOTTER IS CRT,"INTERNAL"
5140  END IF
5150  GRAPHICS ON
5160  X_gdu_max=100*MAX(1,RATIO)
5170  Y_gdu_max=100*MAX(1,1/RATIO)
5180  !--- Title labeling ---
5190  LORG 4                                    !Set ref to top center
5200 !FOR I=-.1 TO .1 STEP .1                   !Creates "bolder" title
5210    MOVE X_gdu_max/2+I,.9*Y_gdu_max         !Move to top center
5220    LABEL T$                                !Label graph
5230 !NEXT I
5240  !--- 1/f parameter labeling
5250  LORG 2
5260  CSIZE 3.5
5270  S$="SV = A/f^B"
5280  A$="A = "
5290  B$="B = "
5300  MOVE .5*X_gdu_max,.8*Y_gdu_max
5310  LABEL S$
5320  MOVE .5*X_gdu_max,.75*Y_gdu_max
5330  LABEL USING "K,D.DDE";A$,A
5340  MOVE .5*X_gdu_max,.7*Y_gdu_max
5350  LABEL USING "K,D.DDD";B$,B
5360  !--- Y axis labeling ---
5370  LORG 4
5380  DEG                                       !Angular unit is degrees
5390  LDIR 90                                   !Rotate label 90 degrees
5400  CSIZE 2.5                                 !Char size=2.5
5410  MOVE .02*X_gdu_max,Y_gdu_max/2            !Move to left center
5420  LABEL Y$                                  !Label y axis
5430  !--- X axis labeling ---
5440  LORG 6                                    !Set ref to bottom
5450  LDIR 0                                    !Rotate label 0 degrees
5460  MOVE X_gdu_max/2,.04*Y_gdu_max            !Move to bottom center
5470  LABEL X$                                  !Label x axis
5480  VIEWPORT .1*X_gdu_max,.9*X_gdu_max,.1*Y_gdu_max,.9*Y_gdu_max
```

Figure A.4 (continued)

```
5490  FRAME                                          !Draw frame around plot
5500  WINDOW Xmin,Xmax,Ymin,Ymax                     !note, units are exponentials
5510  CLIP OFF                                       !allow labeling outside plot
5520  !--- Draw logarithmic x axis ---
5530  FOR Decade=Xmin TO Xmax
5540    FOR Units=1 TO 1+8*(Decade<Xmax)
5550      X=Decade+LGT(Units)
5560      MOVE X,(Ymin)                              !Pointer on x axis
5570      DRAW X,(Ymin+Yrange*.02)                   !draw just above x axis
5580    NEXT Units
5590  NEXT Decade
5600  !--- Label x axis units ---
5610  FOR X=Xmin TO Xmax
5620    LORG 6                                       !Set ref center bottom
5630    CSIZE 3                                      !Size 3 for "10"
5640    MOVE X,(Ymin-Yrange*.01)                     !Just below x axis
5650    LABEL USING "#,K";"10"                       !Compact form for "10"
5660    CSIZE 2                                      !Smaller size for exp
5670    LORG 1                                       !Set ref right top
5680    MOVE (X+Xrange*.02),(Ymin-Yrange*.03)        !Just below and to the right
5690    LABEL USING "#,K";X                          !Compact form for exponent
5700  NEXT X
5710  !--- Draw logarithmic y axis ---
5720  FOR Decade=Ymin TO Ymax
5730    FOR Units=1 TO 1+8*(Decade<Ymax)
5740      Y=Decade+LGT(Units)
5750      MOVE Xmin,Y
5760      DRAW (Xmin+Xrange*.01),Y
5770    NEXT Units
5780  NEXT Decade
5790  !--- Label y axis units ---
5800  FOR Y=Ymin TO Ymax
5810    LORG 8                                       !Set ref to left center
5820    CSIZE 3
5830    MOVE (Xmin-Xrange*.03),Y
5840    LABEL USING "#,K";"10"
5850    CSIZE 2
5860    LORG 4
5870    MOVE (Xmin-Xrange*.03),(Y+Yrange*.01)
5880    LABEL USING "#,K";Y
5890  NEXT Y
5900  !--- Plot data points ---
5910  CLIP OFF
5920  LORG 5
5930  PEN 2                                  !Use plotter pen #2
5940  IF Bfflag=1 THEN                       !Loop for best fit...
5950    FOR I=1 TO Numpts
5960      MOVE LGT(F(I)),LGT(Sv(I))
5970      LABEL USING "A";"*"                !Plot "*" character at each point
5980    NEXT I
5990    !--- Plot best fit ---
6000    CLIP ON
6010    PEN 3                                !Use plotter pen # 3
6020    Y1=(A/(F(1))^B)                      !Calculate Y1 from best fit
6030    Y2=(A/(F(Numpts))^B)                 !Calculate Y2 from best fit
6040    PLOT LGT(F(1)),LGT(Y1)
6050    PLOT LGT(F(Numpts)),LGT(Y2)
6060  ELSE                                   !Loop for no best fit ...
6070    FOR I=1 TO Numpts
```

Figure A.4 (continued)

```
6080      PLOT LGT(F(I)),LGT(Sv(I))
6090    NEXT I
6100  END IF
6110  IF Ptype=1 THEN
6120    PRINT TABXY(1,1),"Hit ""Continue"" when ready"
6130    PAUSE
6140  END IF
6150  IF Ptype=2 THEN
6160    BEEP
6170    PENUP
6180  END IF
6190  GRAPHICS OFF
6200  GCLEAR
6210  SUBEND
```

Figure A.4 (continued)

APPENDIX B

CHARGE-PUMPING MEASUREMENT SYSTEM

Figure B.1 shows a block diagram of the charge-pumping measurement system used in this thesis. The device under test (D.U.T.) is placed inside the HP16058A Test Fixture (this fixture usually accompanies the HP4145 Semiconductor Parameter Analyzer). The computer program listed in Figure B.2 prompts the user for device name, device type (NMOS or PMOS), substrate doping level N_{SUB}, device area and ambient temperature. The HP3314A Function Generator and the Keithley 617 Programmable Electrometer are placed in Remote Mode and programmed by the computer over the GPIB (general purpoe interface bus) to make the necessary measurements. Once the measurements are complete, the program calculates a best fit line to the data and uses the slope of that line to determine D_{it}.

During the measurements, the computer sets the HP3314A function generator's output to an 8 $V_{p\text{-}p}$ 50% duty cycle triangle wave which is applied to the gate of the D.U.T. The voltage source internal to the Keithley 617 Programmable Electrometer applies a reverse bias V_R of 0.5 V to the source/drain to substrate diode. As the computer program increases the triangle wave's frequency from 20 kHz to 200 kHz in 20 kHz steps, the Keithley 617 measures the substrate current I_{CP} at each step. The charge-pumping charge Q_{CP} at each frequency step is then calculated. When all 10 measurements are completed,

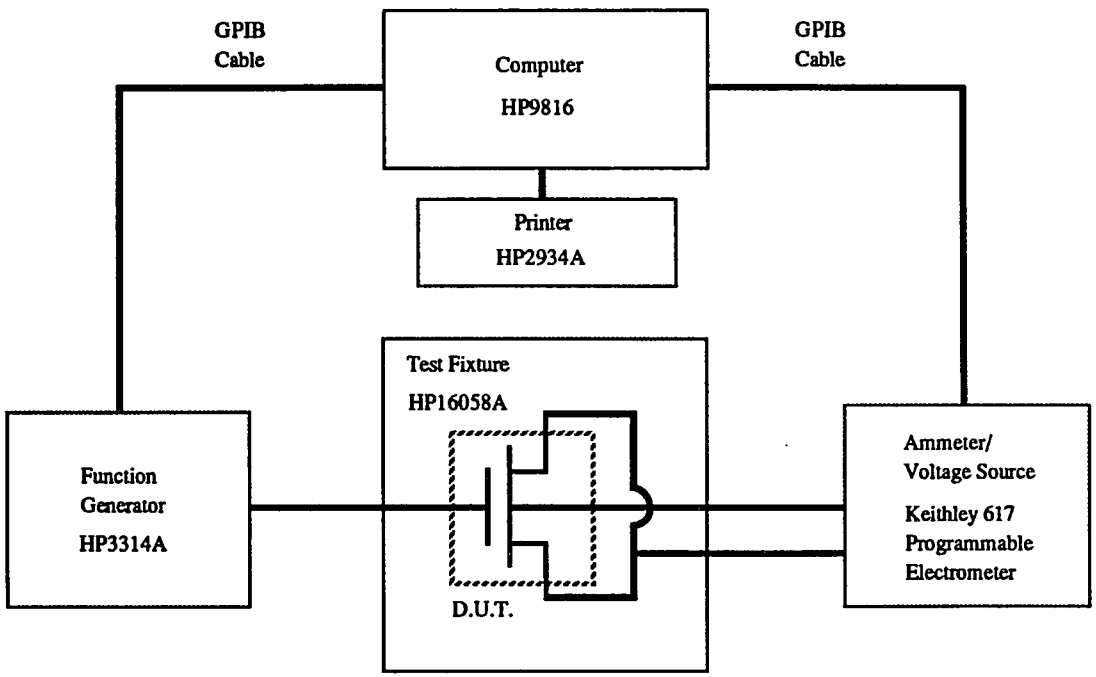

Figure B.1 Charge-pumping measurement system block diagram.

the program calculates the best fit slope of Q_{CP} versus $\ln(f)$ using linear regression. The average interface trap density is calculated using (2.5) as follows:

$$D_{it} = \left|\frac{\partial Q_{CP}}{\partial \ln(f)}\right|\left(\frac{1}{2qkTA_G}\right). \tag{B.1}$$

To account for the space-charge regions around the source and drain, the effective gate area A_G used in (B.1) is calculated using the following one-dimensional model [5]

$$A_G = W\left[L - 2\sqrt{\frac{2\varepsilon_{Si}}{qN_{SUB}}(V_R + \phi_F)}\right] \tag{B.2}$$

where W and L are the drawn width and length dimensions, ε_{Si} is the permittivity of silicon and ϕ_F is the Fermi potential.

```
10   !*************************************************************************
20   !*************************************************************************
30   !**                                                                     **
40   !**      CPUMP                                                          **
50   !**                                                                     **
60   !**      HP Basic 3.0 program for HP9816 computers                      **
70   !**      Extracts average Dit using charge-pumping techniques           **
80   !**                                                                     **
90   !**      Equipment                          GPIB Address                **
100  !**      ---------                          ------------                **
110  !**      HP Func Gen 3314A                      707                     **
120  !**      Keithley Prog. Electrometer 617        727                     **
130  !**                                                                     **
140  !*************************************************************************
150  !*************************************************************************
160  !
170   DIM Name$[40],Title$[50],Line$[70],Afreq$[15]
180   DIM Icp(1:20),Freq(1:20),Qss(1:20)
190   Cls$=CHR$(255)&"K"
200   OUTPUT 2 USING "#,K";Cls$                      !Clear screen
210  !
220  ! ... INPUT USER DATA ...
230   PRINT ""
240   PRINT "   ... CPUMP ..."
250   PRINT ""
260   PRINT "This program measures Dit using charge-pumping measurements"
270   INPUT "Input part name :",Name$
280   INPUT "Input title :",Title$
290   INPUT "Is this an NMOS or PMOS device (N/P) ?",Type$
300   INPUT "Enter the substrate doping level (cm^-3)",Nsub
310   INPUT "Enter Ldrawn and wdrawn in um (separated by a comma):",L,W
320   INPUT "Enter temp in degrees C:",Temp
330   Name$=UPC$(Name$)                              !Convert to upper case
340   Type$=UPC$(Type$)
350   Ld=L*1.E-4                                     !Convert to cm
360   Wd=W*1.E-4
370   T=Temp+273.15                                  !Convert to degrees K
380  !
390  ! ... PRINT CRT MESSAGE ...
400   PRINT ""
410   PRINT ""
420   PRINT "*************************************************"
430   PRINT "***                                           ***"
440   PRINT "***     TAKING CHARGE-PUMP MEASUREMENTS !!!   ***"
450   PRINT "***                                           ***"
460   PRINT "*************************************************"
470   PRINT ""
480  !
490  ! .... CALCULATE VARIABLES ...
500   K=1.38066E-23
510   Q=1.60218E-19
520   Esi=11.9*8.85418E-14
530   Phis=K*T/Q*LOG(Nsub/1.45E+10)
540   Ag=Wd*(Ld-2*(2*Esi/(Q*Nsub)*(.5+2*Phis))^.5)  !Effective gate area
550   Numsteps=10                                    !Number of freq steps
560  !
570  ! ... PRINT INPUT INFO ...
580   PRINTER IS 701
590   PRINT ""
600   PRINT ""
```

Figure B.2 Computer program for charge-pumping measurement system.

```
610   PRINT ""
620   PRINT ""
630   PRINT "Device Name :",Name$
640   PRINT Title$
650   PRINT "Ld,Wd (um) :",L,W
660   PRINT "Effective Gate Area (cm^2) :",Ag
670   PRINT "Nsub (cm^-3) :",Nsub
680   PRINT "Temp (C) :",Temp
690   !
700   ! ... SETUP GPIB EQUIPMENT ...
710   REMOTE 727
720   OUTPUT 727;"F1XR1XC1XZ1X";
730   OUTPUT 727;"R0X00X";
740   IF Type$[1,1]="P" THEN                          !S&D to substrate rev. bias
750     OUTPUT 727;"V-0.50X01X"
760   ELSE
770     OUTPUT 727;"V00.50X01X";
780   END IF
790   OUTPUT 727;"D0XC0X";
800   !
810   REMOTE 707
820   OUTPUT 707;"FU0";
830   OUTPUT 707;"AP00000008.00V0";                   !8 V p-p triangle wave
840   !
850   ! ... BEGIN LOOPING FREQUENCIES ...
860   PRINT ""
870   PRINT " Freq      I charge-pump        Q charge-pump"
880   PRINT " ----      -------------        -------------"
890   Afreq$="FR000000020.0KZ"
900   FOR Fstep=1 TO Numsteps
910     Freq(Fstep)=Fstep*2.E+4                       !20 KHz steps
920     OUTPUT 707;Afreq$;
930     OUTPUT 707;"FU3";
940     OUTPUT 727;"B0X";
950     WAIT 6                                        !Allow readings to stabalize
960     ENTER 727;Raw$
970     FOR Sampleb=1 TO 12
980       Aicp$[Sampleb]=Raw$[Sampleb+4]
990     NEXT Sampleb
1000    Icp(Fstep)=VAL(Aicp$)
1010    Qss(Fstep)=ABS(Icp(Fstep)/Freq(Fstep))
1020    PRINT Freq(Fstep),Icp(Fstep),Qss(Fstep)
1030    IF (NUM(Afreq$[10])<>NUM("8")) THEN
1040      Afreq$[10]=CHR$(NUM(Afreq$[10])+2)
1050      Afreq$=Afreq$&"0.0KZ"
1060    ELSE
1070      Afreq$[9]=CHR$(NUM(Afreq$[9])+1)
1080      Afreq$=Afreq$&"00.0KZ"
1090    END IF
1100    NEXT Fstep
1110    !
1120    ! ... TURN OFF GPIB EQUIPMENT ...
1130    OUTPUT 707;"FU0";
1140    OUTPUT 727;"00X";
1150    !
1160    ! ... CALCULATE BEST FIT PARAMETERS ...
1170    Xsum=0
1180    Ysum=0
1190    Ssxx=0
1200    Ssyy=0
1210    Ssxy=0
```

Figure B.2 (continued)

```
1220   FOR I=1 TO Numsteps
1230     Xsum=Xsum+LGT(Freq(I))
1240     Ysum=Ysum+(Qss(I))
1250   NEXT I
1260   Xbar=Xsum/Numsteps
1270   Ybar=Ysum/Numsteps
1280   FOR I=1 TO Numsteps
1290     Ssxx=Ssxx+(LGT(Freq(I))-Xbar)^2
1300     Ssyy=Ssyy+(Qss(I)-Ybar)^2
1310     Ssxy=Ssxy+((LGT(Freq(I))-Xbar)*(Qss(I)-Ybar))
1320   NEXT I
1330   Slope=Ssxy/Ssxx
1340   Offset=Ybar-Slope*Xbar
1350   R=Ssxy/SQR(Ssxx*Ssyy)
1360   Dit=Slope*LGT(2.718281828846)/(2*K*T*Ag)
1370   PRINT ""
1380   PRINT "Slope :",Slope,"Offset :",Offset
1390   PRINT "Correlation Coeff. :",R
1400   PRINT ""
1410   PRINT "Device Name :",Name$,"Dit :",Dit
1420   PRINT ""
1430   PRINT ""
1440   PRINT ""
1450   PRINT ""
1460   PRINTER IS 1
1470   PRINT ""
1480   PRINT ""
1490   PRINT "Device name :",Name$
1500   PRINT "Dit :",Dit
1510   BEEP
1520   INPUT "hit ""ENTER"" to re-run program ..",Dummy$
1530   GOTO 200
1540   END
```

Figure B.2 (continued)

REFERENCES

[1] B.E. Deal, "The Current Understanding of Charges in the Thermally Oxidized Silicon Structure," *J. Electrochem. Soc.*, vol. 121, p. 198C, 1974.

[2] E.H. Nicollian and J.R. Brews, *MOS Physics and Technology*, New York: J. Wiley & Sons, 1982.

[3] R.F. Pierret, *Field Effect Devices*, 2nd Edition, Vol. IV in *Modular Series on Solid State Devices*, Reading, MA: Addison-Wesley Publ. Co., 1990.

[4] J.S. Brugler and P.G.A. Jespers, "Charge pumping in MOS devices," *IEEE Trans. Electron Devices*, vol. ED-16, p. 297, 1969.

[5] G. Groeseneken, H.E. Maes, N. Beltran, and R.F. De Keersmaecker, "A Reliable Approach to Charge-Pumping Measurements in MOS Transistors," *IEEE Trans. Electron Devices*, vol. ED-31, p. 42, 1984.

[6] S.M. Sze, *Physics of Semiconductor Devices*, 2nd Edition, New York: J. Wiley & Sons, p. 446, 1981.

[7] R.J. Van Overstraeten, G. Declerck, and P.A. Muls, "Theory of the MOS Transistor in Weak Inversion," *IEEE Trans. Electron Devices*, vol. ED-22, p. 282, 1975.

[8] J.B. Johnson, "The Schottky Effect in Low Frequency Circuits," *Phys. Rev.*, vol. 26, p. 71, 1925.

[9] T. Musha, "1/*f* Fluctuations in Biological Systems," *Proc. 6th Int. Conf. on Noise in Physical Systems held at the National Bureau of Standards, Gaithersburg, MD, April 6-10*, p. 143, 1981.

[10] M. Gardner, "White and Brown Music, Fractal Curves and One-Over-*f* Fluctuations," *Scientific American*, vol. 238 (4), p. 16, 1978.

[11] A.L. McWhorter, "1/*f* Noise and Germanium Surface Properties," in *Semiconductor Surface Physics*, Philadelphia: University Press, p. 207, 1957.

[12] S. Christensson, I. Lundstrom, and C. Svensson, "Low Frequency Noise in MOS Transistors - I. Theory," *Solid-St. Electron.*, vol. 11, p. 797, 1968.

[13] G. Blasquez and A. Boukabache, "Origins of 1/*f* Noise in MOS Transistors," in *Noise in Physical Systems and 1/f Noise*, Ed. by M. Savelli, G. Lecoy, and J-P Nougier, Amsterdam: Elsevier Science Publishers B.V., p. 303, 1983.

[14] C. Surya and T.Y. Hsiang, "Theory and Experiments on the $1/f^{\gamma}$ Noise in P-Channel Metal-Oxide-Semiconductor Field Effect Transistors at Low Drain Bias," *Phys. Rev. B*, vol. 33, p. 4898, 1986.

[15] Z. Celik-Butler and T.Y. Hsiang, "Spectral Dependence of $1/f^{\gamma}$ Noise on Gate Bias in N-MOSFETs," *Solid-St. Electronics*, vol. 30, p. 419, 1987.

[16] F.N. Hooge, "1/*f* Noise is No Surface Effect," *Phys. Lett. A*, vol. 29, p. 139, 1969.

[17] M.J. Buckingham, *Noise in Electronic Devices and Systems*, Chichester, England: Ellis Horwood Limited, p. 160, 1983.

[18] C. Surya and T.Y. Hsiang, "Surface Mobility Fluctuations in Metal-Oxide-Semiconductor Field-Effect Transistors," *Physical Review*, vol. 35, p. 6343, 1987.

[19] R. Jayaraman and C.G. Sodini, "A 1/*f* Noise Technique to Extract the Oxide Trap Density Near the Conduction Band Edge of Silicon," *IEEE Trans. Electron Devices*, vol. 36, p. 1773, 1989.

[20] M. Lenzlinger and E.H. Snow, "Fowler-Nordheim Tunneling into Thermally Grown SiO_2," *J. Appl. Phys.*, vol. 40, p. 278, 1969.

[21] M.S. Liang and C. Hu, "Electron Trapping in Very Thin Thermal Silicon Dioxide," *IEDM Tech. Dig.*, p. 396, 1981.

[22] Z.A. Weinberg, "On Tunneling in Metal-Oxide-Silicon Structures," *J. Appl. Phys.*, vol. 53, p. 5052, 1982.

[23] I.C. Chen, S. Holland, and C. Hu, "Oxide Breakdown Dependence on Thickness and Hole Current - Enhanced Reliability of Ultra Thin Oxides," *IEDM Tech. Dig.*, p. 660, 1986.

[24] Y.B. Park, M.S. Thesis, University of Arizona, 1992.

[25] G. Gritt, "Charge Pumping Studies of MOSFET Transistors Subject to Various Levels of Copper Contamination," Senior Project Report, University of Arizona Department of Electrical and Computer Engineering, 1992.

[26] M.-S. Liang, C. Change, Y. Tong, C. Hu, and R.W. Brodersen, "MOSFET Degradation Due to Stressing of Thin Oxides," *IEEE Trans. Electron Devices*, vol. ED-31, p. 1238, 1984.

[27] Y. Nissan-Cohen, J. Shappir, D. Frohman-Bentchkowsky, "High Field Current Induced-Positive Charge Transients in SiO_2," *J. Appl. Phys.*, vol. 54, p. 5793, 1983.

[28] S.C. Witczak, J.S. Suehle, and M. Gaitan, "An Experimental Comparison of Measurement Techniques to Extract Si-SiO_2 Interface Trap Density," *Solid-St. Electron.*, vol. 35, p. 345, 1992.

[29] F.M. Klaassen, "Characterization of Low $1/f$ Noise in MOS Transistors," *IEEE Trans. Electron Devices*, vol. ED-18, p. 887, 1971.

[30] G. Broux, R. Van Overstraeten, and G. Declerck, "Experimental Results on Fast Surface States and $1/f$ Noise in M.O.S. Transistors," *Electron. Lett.*, vol. 11, p. 97, 1975.

[31] T.L. Meisenheimer and D.M. Fleetwood, "Effects of Radiation-Induced Charge on $1/f$ Noise in MOS Devices," *IEEE Trans. Nucl. Sci.*, vol. NS-36, p. 1696, 1990.

[32] T.L. Meisenheimer, D.M. Fleetwood, M.R. Shaneyfelt, and L.C. Riewe, "$1/f$ Noise in N- and P-Channel MOS Devices Through Irradiation and Annealing," *IEEE Trans. Nucl. Sci.*, vol. NS-38, p. 1297, 1991.

[33] P. Augier, J.L. Todsen, D. Zupac, R.D. Schrimpf, K.F. Galloway, J.A. Babcock, "Comparison of 1/*f* Noise in Irradiated Power MOSFETs Measured in the Linear and Saturation Regions," submitted to *IEEE Trans. Nucl. Sci.*

[34] D.K. Schroder, *Semiconductor Material and Device Characterization*, New York: John Wiley & Sons, p. 268, 1990.